RSC Sustainability

ROYAL SOCIETY OF CHEMISTRY

PAPER

View Article Online
View Journal

Cite this: DOI: 10.1039/d6su00302h

Optimization of a CALB catalyzed esterification process for the synthesis of methyl glucoside fatty acid esters: green metrics, application and antimicrobial evaluation

Abinash Nayak, [a] Luana Carnaval, [b] Swarna Jaiswal, [b] Julie L. Dunne, *[c] Michael Kinsella [a] and Claire M. Lennon *[d]

Carbohydrate fatty acid esters (CFAE) are promising sustainable antimicrobials with potential therapeutic applications. Although enzymatic synthesis of CFAE offers advantages, issues such as substrate solubility, limited exploration of non-classical greener solvents, additional synthetic steps, and analytical challenges hinder applicability and scale-up. In addition, mono-protected monosaccharide/unsaturated fatty acid (uFA) based CFAE are underexplored for antimicrobial evaluation. Our study systematically investigated the *Candida antarctica* lipase B (CALB) catalyzed esterification of methyl α-D-glucopyranoside (MAG) and lauric acid (LA) as a model system, employing green chemistry concepts to generate a panel of potentially more sustainable antimicrobial products. Systematic reaction optimization was followed by its application to generate 18 mono-substituted CFAE, including 7 novel derivatives. Among the screened solvents, propylene carbonate (PC) and ethylene carbonate (EC) yielded 59% and 56% of monoester product, respectively. Under optimized conditions (MAG : LA – 1 : 3 equivalence), acetonitrile afforded the highest yield of 89% in 4 h at 60 °C. An enzyme reusability study showed reduction of activity when the recovered biocatalyst was dried, while direct reuse with added drying agent maintained activity over 7 cycles. In the gram-scale synthesis of MAG monolaurate (**3a**), recovery of unreacted LA through the non-chromatographic workup improved the reaction mass efficiency (RME) from 39.53% to 83.19%. Solvent parameter analysis using polarity, log *P* and Kamlet–Taft values, and green metric evaluation, through the EcoScale and CHEM21 first-pass toolkits were undertaken. These identified clear areas for further improvement. A screening cradle-to-gate Life Cycle Assessment was completed using SimaPro®, identifying auxiliary energy demand and solvent use as environmental hotspots within our study. Antimicrobial evaluation against the Gram-positive *Staphylococcus aureus* (ATCC 25923) identified monooleate of methyl β-D-glucopyranoside (MBG monooleate, **4e**) as the most active CFAE, with MIC and MBC values of 0.0156 mM, corresponding to ~32-fold improvement in inhibitory potency compared to oleic acid with MIC and MBC at 0.5000 mM.

Received 26th May 2026
Accepted 17th June 2026

DOI: 10.1039/d6su00302h

rsc.li/rscsus

Sustainability spotlight

This work presents an enzymatic esterification to produce bioactive CFAE, underutilized yet potentially more sustainable antimicrobials, with food, pharmaceutical, and packaging applications. A sustainability mindset was undertaken, and green chemistry concepts were applied across the reaction process, including using potentially renewable and reusable substrates and catalyst, assessing greener solvents, milder reaction conditions, minimization of solvent, single step synthesis, with low dependence on chromatography in purification and analysis. The aim was to develop a process to generate a panel of CFAE as novel antimicrobials to support UN SDG 3 (Good Health and Well-Being), produced through methods aligning with UN SDG12 (Responsible Consumption and Production). In the context of CFAE, for the first time, to our knowledge, the process was evaluated by EcoScale and CHEM21 first-pass toolkits. Developing novel bio-based antimicrobials potentially contributes to innovation in health, food, pharmaceutical, and packaging industries contributing to SDG9 (Industry, Innovation and Infrastructure), and greener synthetic approaches may help to reduce carbon footprints, supporting SDG 13 (Climate action). The complete approach demonstrates how process development at the early bench stage can contribute to process understanding and enable effective synthesis of beneficial compounds. The approach also contributes to researcher education in this area.

[a]*Pharmaceutical and Molecular Biotechnology Research Centre (PMBRC), Department of Science, Faculty of Science and Computing, South East Technological University, Cork Road, Waterford City, Co. Waterford, X91 K0EK, Ireland*

[b]*Centre for Sustainable Packaging and Bioproducts, School of Food Science and Environmental Health, Technological University Dublin, Park House Grangegorman, 191 North Circular Road, D07 EWV4, Ireland*

[c]*School of Food Science and Environmental Health, Technological University Dublin, Park House Grangegorman, 191 North Circular Road, D07 EWV4, Ireland. E-mail: Julie.Dunne@tudublin.ie*

[d]*Pharmaceutical and Molecular Biotechnology Research Centre (PMBRC), Department of Pharmacy, Faculty of Science and Computing, South East Technological University, Cork Road, Waterford City, Co. Waterford, X91 K0EK, Ireland. E-mail: Claire.Lennon@setu.ie*

Introduction

Carbohydrate fatty acid esters (CFAE) are widely reported as biodegradable, non-ionic, non-toxic, and odorless biosurfactants with applications in the pharmaceutical, food, and cosmetic industries.[1–4] Carbohydrate fatty acid monoesters have been synthesized by both chemical[1,5,6] and enzymatic methods, including glucose-derived monoesters.[7–11] Several studies have reported their antimicrobial evaluation, demonstrating these versatile compounds as functional surfactants and promising alternatives to address antimicrobial resistance.[5–9,11,12] Enzymatic synthesis of these amphiphilic compounds supports several green chemistry principles and promotes sustainable synthesis,[13,14] by reducing multiple protection and deprotection steps and avoiding associated hazardous reagents and solvents.[1–4,10,15–17] It also offers potential for a wider range of compounds to be synthesised and assessed, particularly unsaturated fatty acids (uFAs), which may be degraded by conventional chemical methods. For example, hydrogenation to remove *O*-benzyl (OBn) protecting groups can pose risks of double-bond reduction or formation of undesired *trans*-fatty acid (FA) products.[18,19]

Although enzymatic synthesis of CFAE has been presented in literature for over two decades and can be considered a relatively "green" method, consistent access to isolated quantities of structurally diverse CFAE remains challenging. Key limitations, from our perspective, include limited investigation of greener solvents and the need for robust analytical methods that can quantify crude reaction mixtures during development, and facilitate mass-based yield determination. In addition, process sustainability metrics for isolated CFAE products are rarely reported, limiting direct comparison between protocols. Our aim for this work was to generate a series of monosaccharide-based CFAE, and to complete structure–activity relationship (SAR) analysis to identify novel antimicrobials. We sought to complete this with a green chemistry and sustainability mindset, in the generation of these analogues in our laboratory, seeking to optimize the process we employed. This required a holistic assessment of an enzymatic method of synthesizing the CFAE analogues, beginning with a model esterification reaction of MAG (**1a**), as a common relatively simple monosaccharide glycoside, and lauric acid (**2a**), recognized as one of the most active medium chain FAs,[20] with the view to comprehensively understanding process variabilities, challenges, and precedents. It was our aim with this assessment complete, to apply the developed method to prepare a range of CFAE based on medium to long chain unsaturated fatty acids and monosaccharide methyl glycosides. We also wished to avoid the alternative transesterification process, given the requirement for additional steps in synthesis of the fatty acid ester substrate, possible by-products, and aiming for minimal application of flash chromatography, a challenge in carbohydrate synthetic methods.[1]

Historically, organic solvents such as acetone, *tert*-butanol (*t*-BuOH), *n*-hexane, toluene, dioxane, acetonitrile (MeCN), dimethyl sulfoxide (DMSO), dimethylformamide (DMF), tetrahydrofuran (THF), pyridine,[1,21–29] and 2-methyl-2-butanol (2M2B)[1,29–31] have been part of enzymatically catalyzed CFAE synthesis. In recent years, a series of dipolar aprotic and bio-derived solvents have been classified as safer, greener, and potentially more sustainable alternatives for many chemical and enzymatic applications.[32–34] Several offer potential as alternatives to hazardous solvents such as DMF, *N*,*N*-dimethylacetamide (DMAc), *N*-methyl-2-pyrrolidone (NMP), 1,4-dioxane, THF, and diethyl ether.[35–37]

Alternative greener solvents have been investigated in many conventional chemical reactions, including solvents from the carbonate family,[36,38] such as the acyclic carbonates dimethyl carbonate (DMC) and diethyl carbonate (DEC) and the cyclic carbonates propylene carbonate (PC) and ethylene carbonate (EC). Cyclopentyl methyl ether (CPME)[39] and 2-methyltetrahydrofuran (2-MeTHF),[40,41] dipolar aprotic solvents such as dimethyl isosorbide (DMI),[42] γ-valerolactone (GVL),[43] and dihydrolevoglucosenone (Cyrene™)[44,45] as well as renewable hydrocarbons such as limonene, have been applied.[46] In CALB catalysed esterification reactions, 2-MeTHF, Cyrene™, CPME, and PC have been assessed.[41,45,47,48] Our study focused on exploring these solvents in the CALB-catalyzed esterification of MAG (**1a**) with LA (**2a**), assessing their impact on solubility, yield and regioselectivity. The physicochemical properties of solvents (polarity, log *P*, Kamlet–Taft parameters) were also compared with reaction outcome (yield) to identify trends relevant to CFAE synthesis. This study also incorporated further elements of development with the aim of reducing reaction time, determining optimum temperature, loading of molecular sieves, molar equivalents of components, catalyst quantity, and enzyme recycling. Within CFAE synthetic protocols, the use of biological incubator shakers is also common,[8,49–52] however we wished to employ standard chemical laboratory equipment and heating method (oil-bath) as an alternative.

In CFAE synthesis, the establishment of a robust analytical method is crucial. The ^{1}H quantitative NMR (^{1}H qNMR) analytical method developed and applied in this work was systematically validated within the optimized process and published by our group in 2024, to highlight the usefulness and underutilized application of qNMR in CFAE synthesis.[53] The ^{1}H qNMR method using CD_3OD and fumaric acid (FA) as internal standard (IS) allowed quantification of all reaction components in the crude by mass, and therefore could be applied to calculate product yield. All parameters including selectivity, linearity, accuracy, precision, robustness, LOD, and LOQ for the method using CD_3OD and FA were validated,[54,55] where accuracy for all analytes (MAG (**1a**), LA (**2a**), and MAG monolaurate (**3a**)) across tested concentration levels was higher than 98.29%, corresponding to 100 ± 2% error.[53] The applicability was confirmed by comparison with isolated yields obtained post purification, showing <3% deviation between ^{1}H qNMR determined and isolated yields. The work presented in this manuscript details systematic reaction optimization, applying this method of analysis to support reaction profiling and yield determination.

The CHEM21 toolbox (Chemical Manufacturing Methods for the 21st Century Pharmaceutical Industries) supports greener process development by assessing parameters such as mass

efficiency, solvent selection, safety, energy use, and purification.[56] In parallel, EcoScale is a semiquantitative, post-synthetic analysis tool, designed to assess and penalize parameters such as yield, reagent cost, safety, reaction conditions and purification, based on their adverse effects on safety, cost-effectiveness, and environmental impact.[57] A score >75 out of 100 is classified as an "excellent synthesis" as per the EcoScale evaluation criteria, guiding the researcher to improve or innovate to meet this target. This approach offers a quick assessment of reaction efficiency while the CHEM21 first-pass tool kit provides a more comprehensive comparative framework only for early-stage process development. In our work, the EcoScale and CHEM21 first-pass toolkit were applied to evaluate the optimized CFAE synthetic process as we worked at bench scale, and these are therefore discussed in this context. Additionally, to capture environmental, health, and safety impacts associated with material and energy inputs, life cycle assessment (LCA) can provide insights to environmental impact by assessing resource consumption and waste generation.[58,59] LCA can identify hotspots such as energy demand, solvent use, and purification operations that may not be fully reflected by mass-based green metrics alone. In this work, a screening cradle-to-gate LCA was also included to identify environmental hotspots for the gram-scale synthesis of MAG monolaurate (**3a**).

Esterification reactions to form CFAE derivatives of alkyl (methyl, ethyl, isopropyl, *n*-propyl, *n*-butyl) glucosides, using saturated fatty acids (C_6–C_{18}) have been explored in detail in the literature.[50–52,60–64] However, unsaturated fatty acids (uFAs) are less studied as substrates in these reactions and hence as CFAE components. Mutschler *et al.* reported the lipase (CALB/Novozym 435) catalyzed synthesis of methyl 6-*O*-alkanoyl-α-D-glucopyranosides from oleic acid ($C_{18:2}$) and saturated fatty acids.[52] In a study by Bousquet *et al.*, three unsaturated fatty acid esters of butyl α-D-glucopyranoside were prepared from oleic acid ($C_{18:1}$), linoleic acid ($C_{18:2}$), and linolenic acid ($C_{18:3}$) for dermo-cosmetic applications.[65] In our work, the optimized enzymatic method was applied to a series of uFAs and methyl α/β-D-glucopyranoside. The CFAE generated were assessed for their antimicrobial activities against the Gram-positive organism *Staphylococcus aureus* (ATCC 25923). The selection of uFAs (C_{10}–C_{20}) and their effect on the yield of products in synthesis and on antimicrobial activity was assessed.

Materials and methods

Materials

Methyl α-D-glucopyranoside (**1a**, ≥99%, Sigma-Aldrich), methyl β-D-glucopyranoside (**1b**, ≥99%, Sigma-Aldrich), lauric acid (**2a**, 99.5%, Sigma-Aldrich), 9-decenoic acid (**2b**, 99.6%, Fluorochem), 2-undecenoic acid (**2c**, 70%, tech grade, Fluorochem), 10-undecenoic acid (**2d**, 99.89%, Fluorochem), oleic acid (**2e**, 99%, ThermoFisher Scientific), elaidic acid (**2f**, ≥90%, Fluorochem), linoleic acid (**2g**, 96.34%, Fluorochem), linolenic acid (**2h**, 74.8%, Fluorochem), arachidonic acid (**2i**, 94.64%, Fluorochem), Novozym 435/CALB (≥5000 U g^{-1}, Sigma-Aldrich), molecular sieves (3 Å, 1–2 mm/10–18 mesh beads, ThermoFisher Scientific), and solvents were obtained commercially from Sigma Aldrich, Fluorochem, and ThermoFisher Scientific. Molecular sieves (3 Å) were activated in an oven at 150 °C overnight prior to use. LC-MS grade solvents were used for HR-MS data with >99% purity. Fumaric acid (FA, 99%, Fluorochem) as internal standard was used for the ^{1}H qNMR analytical method using deuterated methanol (CD_3OD, 99.8%, Fluorochem). Precision NMR tubes (Wilmad 526-PP-7, Sigma-Aldrich) were used for all ^{1}H qNMR analyses. MeCN (Honeywell, HPLC grade, CHROMASOLV™, ≥99.9%) was used as received, with a certified water content (Karl Fischer titration) of <0.001% (w/w). Additional water content analysis was not performed. For all solvent screening reactions, no additional drying or water content adjustment was carried out prior to use.

For ^{1}H qNMR quantitation, an XPE 56 microbalance (Mettler Toledo, USA) was used for mass measurement with a resolution of 0.001 mg and validated by measuring certified reference weights of 10 and 100 mg using internal calibration available in the balance. A 100–1000 μL pipette (Labnet) was routinely checked for accuracy prior to experimental use.[53] A JEOL JNM-ECX 400 MHz spectrometer (JEOL, Tokyo, Japan) with a 5 mm liquid ROYALPROBE was used for NMR, operating at 9.389T, 399.7907 MHz for ^{1}H and 101 MHz for ^{13}C with Delta operating software version 4.3.6. Prior to spectra acquisition, the NMR probe was auto-tuned and matched. All ^{1}H qNMR acquisition parameters were applied as per the previously published and validated protocol.[53] For the ^{1}H qNMR yield determination, NMR spectra were processed in JEOL Delta data analysis software version 6.1.0. and for NMR characterization data of isolated compounds (^{1}H and ^{13}C), spectra were processed in JEOL JASON software version 5.2.9369. The HRMS data were acquired using Agilent 6545B LC/Q-TOF and analyzed using MassHunter software. Melting points were analyzed by Differential Scanning Calorimetry (DSC) using DSC 214 Polyma instrument (NETZSCH, Selb, Germany) with operating software Proteus Thermal analysis 8.0.3. Samples (3–5 mg) in aluminium pans (Concavus® Al, pierced lids) were heated from 0–150 °C at 10 K min^{-1} under nitrogen to determine the melting point.

General procedure for enzymatic esterification of methyl glucosides with fatty acids (3a–i and 4a–i)

Methyl α-D-glucopyranoside/MAG (**1a**) or methyl β-D-glucopyranoside/MBG (**1b**) (50 mg, 0.26 mmol, 1 equiv.), fatty acids (**2a–i**, 3 equiv.), lipase (immobilized CALB/Novozym 435, 50 wt% of **1a** or **1b**) and molecular sieves 3 Å (80 wt% of **1a** or **1b**) were placed in an oven-dried 7 mL glass vial. This was followed by the addition of 3 mL of MeCN. The reaction mixture was stirred (magnetic stirrer) in an oil-bath setup and maintained at 60 °C and 100 rpm for 4 h. Reactions were analyzed by TLC with 100% EtOAc as the eluent and plates were visualized by dipping in a carbohydrate stain (95 : 5 v/v% of EtOH : H_2SO_4) followed by exposure to a hotplate at 150 °C. The enzyme and molecular sieves were filtered, which was followed by a 15 mL MeOH wash of the residue. The combined filtrate and wash were evaporated under reduced pressure at 30 °C to obtain the reaction crude. The crude was subjected to quantitative NMR analysis and/or the purification procedure as outlined in the next section.

Purified products were subsequently characterized by ^{1}H and ^{13}C NMR, HRMS, and DSC for melting point of solid monoesters.

Enzyme recycling procedure

For the enzyme recycling study, the Novozym 435 and molecular sieves were filtered and removed from the reaction mixture. The solid was first washed with 10 mL of MeCN (the reaction solvent) and manually collected from the filter paper. This was followed by a wash of the filter paper with 10 mL of MeOH to ensure the complete recovery of reaction components, particularly unreacted carbohydrate *i.e.*, MAG (**1a**). For each subsequent reaction cycle, freshly activated 3 Å molecular sieves were added, and the Novozym 435 was reused.

^{1}H qNMR method for yield determination from the dried reaction crude[53]

After drying under reduced pressure, the crude was weighed, before being completely dissolved in *ca.* 10 mL of MeOH. A 1 mL aliquot was transferred to a pre-weighed round-bottomed flask (5 or 10 mL) and dried *in vacuo* to obtain a representative crude sample for ^{1}H qNMR analysis. This process was repeated to prepare duplicate samples. The mass of the crude sample was recorded on a calibrated micro balance. This was followed by the addition of a small quantity of fumaric acid (internal standard) directly to the round-bottomed flask containing the crude sample. The mass of added fumaric acid was recorded. The resultant complete sample was dissolved in 0.8 mL of CD_3OD and transferred to a clean, dry NMR tube. Each sample was analyzed in duplicate by NMR. The ^{1}H NMR spectra were acquired using a 90° pulse angle, a relaxation delay of 32 s to ensure complete relaxation and ≥16 scans to gain adequate signal-to-noise (SNR), with further instrumental and processing parameters included in our previous publication.[53]

Where yield was determined using ^{1}H qNMR, the product mass % purity in the accurately weighed crude was calculated from the following parameters: signal integrals, sample mass, added internal standard mass and its purity, applying the established absolute ^{1}H qNMR method (refer to Section 1 in SI for yield calculation).[53,55,66] This allowed determination of the % mass purity and hence the total mass of product within the reaction crude. This mass was compared to the theoretical yield of the limiting reagent (MAG, **1a**) to determine % yield of product.

Where alternatively isolated product was obtained, post the purification step, this was confirmed by characterization, and the actual mass used to determine yield. The purity of all isolated compounds was assessed by ^{1}H qNMR, with the purity of representative compounds detailed in the SI (Section 13).

To assess intra-laboratory precision of the reaction yield, the relative standard deviation (RSD) was calculated for five independent experiments performed under identical reaction conditions of MAG (**1a**, 50 mg/0.26 mmol, 85.83 mM): LA (**2a**, 2 equiv.) in MeCN, Novozym 435–50 wt% of **1a**, 3 Å MS – 80 wt% of **1a** at 60 °C, 4 h and 100 rpm, including three experiments from the optimization and two from the enzyme recycling study. The RSD of the analytically measured ^{1}H qNMR yield was calculated using the following eqn (1), where σ is the standard deviation and AY is the average yield of product (**3a**) for the five different experiments:[53]

$$\mathrm{RSD}(\%) = \left(\frac{\sigma}{\mathrm{AY}}\right) \times 100 \quad (1)$$

General procedure for purification of 3a, 3b, 3f, 4a, 4b and 4f[53]

After measuring the mass of the reaction crude, the mixture was partitioned between an aqueous and EtOAc phase in a 1 : 2 (v/v) ratio. The aqueous phase containing unreacted carbohydrate was separated and extracted further with EtOAc to ensure carbohydrate was removed and this process was monitored by TLC. The combined collected organic phase (EtOAc) was dried over Na_2SO_4 and concentrated *in vacuo* to produce a mixture containing monoester and unreacted fatty acid. Trituration of this residue with *n*-heptane dissolved the fatty acid and provided the monoester product as white solid precipitate. The product was collected by filtration, washed with *n*-heptane and dried under reduced pressure prior to characterization. The filtrate (*n*-heptane) was concentrated *in vacuo* to recover the unreacted fatty acid, and both CFAE product and recovered fatty acid were analyzed by ^{1}H NMR.

General preparative TLC procedure for purification of 3c, 3d, 3e, 3g, 3h, 3i, 4c, 4d, 4e, 4g, 4h and 4i

The reaction crude was dissolved in 2–3 mL of MeOH and applied as a continuous band to a preparative TLC plate (20 × 20 cm, silica gel with fluorescent tracer, UV 254). The TLC plate was eluted with 100% EtOAc, removed, dried, and visualized under UV light for CFAE products (**3e**, **3g**, **3h**, **3i**, **4e**, **4g**, **4h** and **4i**). The silica gel band corresponding to the product was removed and the component was extracted with EtOAc (2 × 10 mL). The combined extracts were filtered to remove silica and concentrated *in vacuo* to obtain isolated product. For UV inactive products (**3c**, **3d**, **4c** and **4d**), the product band was identified by comparison with a stained parallel TLC, where the product spot was visualized and its retention factor (R_f) was determined, and the corresponding band was collected. The characterization data (melting point, ^{1}H, ^{13}C, and high-resolution LC-MS) for the novel CFAE are provided along with details for previously published products in the SI.

Screening cradle-to-gate life cycle assessment (LCA)

A model screening cradle-to-gate LCA was performed to evaluate the environmental impacts associated with the gram-scale synthesis of MAG monolaurate (**3a**) using SimaPro® 10.3.0.3 software. Background data were obtained from the Ecoinvent v3.11 database (allocation, cut-off system model). The functional unit was defined as 1 g of isolated MAG monolaurate (**3a**). The life cycle inventory was constructed from the experimentally isolated batch (1.89 g of isolated CFAE product **3a**) and implemented in SimaPro® as the reference flow, with results scaled to the functional unit of 1 g of **3a**. The system boundary

included raw material production, using proxy datasets where specific data was unavailable, solvent use, electricity consumption, and purification steps up to the point of product isolation (cradle-to-gate) (Fig. 1). Waste streams generated during the synthesis and purification stages were treated within the system boundary using appropriate wastewater treatment and hazardous waste incineration datasets.

The life cycle inventory (LCI) was constructed using primary experimental data from the gram-scale synthesis of **3a** (SI, Table S13 and S14), including measured quantities of reactants, solvents, auxiliaries, and electricity consumption. The total electricity demand included energy associated with reaction, solvent removal, vacuum drying, and activation of 3 Å molecular sieves. Background datasets were selected from Ecoinvent based on the closest available material or process. Where exact datasets were unavailable, proxy datasets were used based on chemical similarity or simplified production analogues.[67,68] Specifically, MAG (**1a**) production was approximated to glucose production, lauric acid to fatty acid production from palm kernel oil, Novozym 435 to generic enzyme production, and 3 Å molecular sieves to zeolite powder production. These selections represent proxy-based modelling approaches commonly applied to address LCI data gaps.[67]

Environmental impacts were assessed using the ReCiPe 2016 v1.12 (World 2010 H/A, Hierarchist perspective) method as implemented in SimaPro. Endpoint results (expressed in millipoints, mPt) represent aggregated impacts across human health, ecosystem quality, and resource scarcity, and were used to evaluate overall environmental burden and perform contribution analysis, while selected midpoint indicators were used to examine key impact categories.[59]

Methyl 6-*O*-9-decenoyl-α-D-glucopyranoside (3b)

White solid (75 mg, 84% yield). Melting point (DSC): 45.6 °C. ^{1}H NMR (400 MHz, $CDCl_3$): δ 5.80 (m, 1H, $CH_2CH{=}CH_2$, H-9′), 4.96 (m, 2H, $CH_2CH{=}CH_2$, H-10′), 4.77 (d, $J_{1,2}$ = 3.9 Hz, 1H, C**H**OCH$_3$, H-1), 4.49 (dd, $J_{6a,6b;6a,5}$ = 12.1, 4.6 Hz, 1H, C**H**$_2$OCO, H$_a$-6), 4.25 (dd, $J_{6b,6a;6b,5}$ = 12.1, 2.1 Hz, 1H, C**H**$_2$OCO, H$_b$-6), 3.72 (m, 2H, 2×C**H**OH, H-3,5), 3.54 (dd, $J_{2,3;1,2}$ = 9.4, 3.8 Hz, 1H, C**H**OH, H-2), 3.42 (s, 3H, OC**H**$_3$, H-7), 3.32 (apt t, $J_{3,4;4,5}$ = 9.4 Hz, 1H, C**H**OH, H-4), 2.37 (t, $J_{2',3'}$ = 7.6 Hz, 2H, C**H**$_2$CO, H-2′), 2.03 (m, 2H, C**H**$_2$CH=CH$_2$, H-8′), 1.62 (m, 2H, CH$_2$C**H**$_2$CH$_2$, H-3′), 1.29 (m, 8H, 4×C**H**$_2$, H4′–H7′) ppm. ^{13}C NMR (101 MHz, $CDCl_3$): δ 174.4 (**C**=O, C-1′), 139.1 (**C**H=CH$_2$, C-9′), 114.3 (CH=**C**H$_2$, C-10′), 99.5 (C-1), 74.1(C-3), 72.0 (C-2), 70.3 (C-4), 69.8 (C-5), 63.5 (C-6), 55.3 (O**C**H$_3$, C-7), 34.2 (C-2′), 33.8 (C-8′), 29.2, 29.1, 29.0, 28.9 (4 × aliphatic *C*H$_2$, C4′–C7′), 24.9 (C-3′) ppm. HRMS (ESI-MS) *m*/*z* calc. for $C_{17}H_{30}O_7$, $[M + H]^+$ 347.2064, found 347.2063.

Methyl 6-*O*-(9E)-octadecenoyl-α-D-glucopyranoside (3f)

White solid (76 mg, 64% yield). Melting point (DSC): 66.3 °C. ^{1}H NMR (400 MHz, $CDCl_3$): δ 5.37 (m, 2H, $CH_2CH{=}CHCH_2$, H-9′,10′), 4.78 (d, $J_{1,2}$ = 3.8 Hz, 1H, C**H**OCH$_3$, H-1), 4.53 (dd, $J_{6a,6b;6a,5}$ = 12.3, 4.4 Hz, 1H, C**H**$_2$OCO, H$_a$-6), 4.22 (dd, $J_{6b,6a;6b,5}$ = 12.3, 2.2 Hz, 1H, C**H**$_2$OCO, H$_b$-6), 3.72 (m, 2H, 2×C**H**OH, H-3,5), 3.52 (dd, $J_{2,3;1,2}$ = 9.3, 3.6 Hz, 1H, C**H**OH, H-2), 3.43 (s, 3H, OC**H**$_3$, H-7), 3.32 (apt t, $J_{3,4;4,5}$ = 9.3 Hz, 1H, C**H**OH, H-4), 2.37 (t, $J_{2',3'}$ = 7.6 Hz, 2H, C**H**$_2$CO, H-2′), 1.95 (m, 4H, C**H**$_2$CH=CHC**H**$_2$, H-8′,11′), 1.62 (m, 2H, CH$_2$C**H**$_2$CH$_2$, H-3′), 1.25 (m, 20H, 10×C**H**$_2$, H4′–H7′ + H12′–H17′), 0.87 (t, $J_{18',17'}$ = 6.9 Hz, 3H, CH$_2$C**H**$_3$, H-18′) ppm. ^{13}C NMR (101 MHz, $CDCl_3$): δ 174.9 (**C**=O, C-1′), 130.6 (CH=**C**H, C-9′), 130.3 (**C**H=CH, C-10′), 99.4 (C-1), 74.4 (C-3), 72.3 (C-2), 2 × 69.9 (C-4, C-5), 63.0 (C-6), 55.6 (O**C**H$_3$, C-7), 34.2, 2 × 32.7, 32.0, 29.8, 29.7, 29.6, 29.4, 29.3, 2 × 29.2, 29.1, 25.0, 22.8 (14 × aliphatic **C**H$_2$, C2′–C8′ & C11′–C17′), 14.2 (terminal aliphatic **C**H$_3$, C-18′) ppm. HRMS (ESI-MS) *m*/*z* calc. for $C_{25}H_{46}O_7$, $[M + H]^+$ 459.3316, found 459.3320.

Methyl 6-*O*-(5Z,8Z,11Z,14Z)-eicosatetraenoyl-α-D-glucopyranoside (3i)

Transparent viscous liquid (71 mg, 57% yield). ^{1}H NMR (400 MHz, $CDCl_3$): δ 5.36 (m, 8H, $(CH_2CH{=}CHCH_2)_4$, H-5′,6′,8′,9′,11′,12′,14′,15′), 4.75 (d, $J_{1,2}$ = 3.9 Hz, 1H, C**H**OCH$_3$, H-

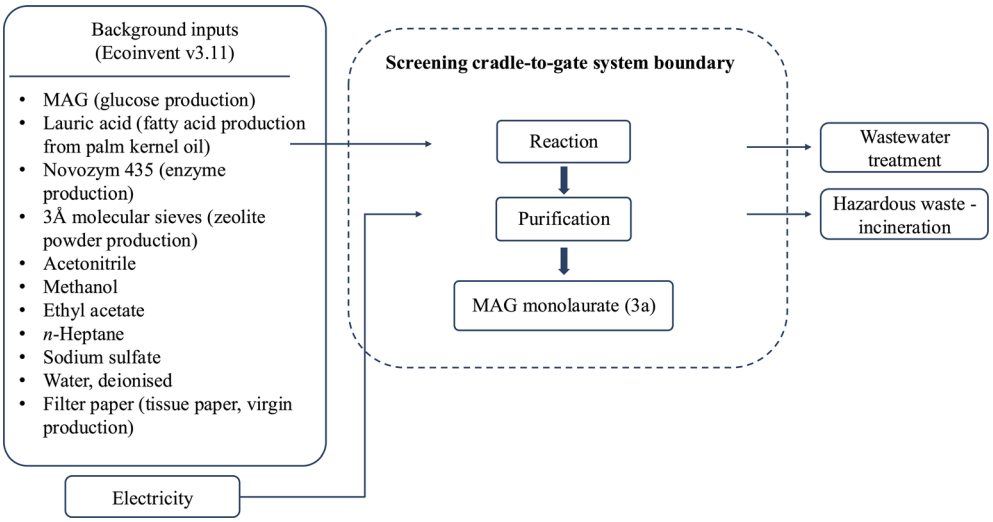

Fig. 1 System boundary for the model screening cradle-to-gate assessment of MAG monolaurate (**3a**).

1), 4.43 (dd, $J_{6a,6b;6a,5}$ = 12.1, 5.0 Hz, 1H, C**H**$_2$OCO, H$_a$-6), 4.28 (dd, $J_{6b,6a;6b,5}$ = 12.1, 2.1 Hz, 1H, C**H**$_2$OCO, H$_b$-6), 3.72 (m, 2H, 2×C**H**OH, H-3,5), 3.51 (dd, $J_{2,3;1,2}$ = 9.5, 3.7 Hz, 1H, C**H**OH, H-2), 3.41 (s, 3H, OC**H**$_3$, H-7), 3.33 (apt t, $J_{3,4;4,5}$ = 9.5 Hz, 1H, C**H**OH, H-4), 2.81 (m, 6H, (CH=CHC**H**$_2$)$_3$CH=CH, H-7′,10′,13′), 2.38 (t, $J_{2',3'}$ = 7.7 Hz, 2H, C**H**$_2$CO, H-2′), 2.08 (m, 4H, C**H**$_2$(CH=CHCH$_2$)$_3$CH=CHC**H**$_2$, H-4′,16′), 1.71 (m, 2H, CH$_2$-C**H**$_2$CH$_2$, H-3′), 1.31 (m, 6H, 3×C**H**$_2$, H-17′,18′,19′), 0.88 (t, $J_{20',19'}$ = 6.8 Hz, 3H, CH$_2$C**H**$_3$, H-20′) ppm. ^{13}C NMR (101 MHz, CDCl$_3$): δ 174.2 (**C**=O, C-1′), 130.5 (C-5′), 129.0 (C-6′), 128.8 (C-8′), 128.6 (C-9′), 128.3 (C-11′), 128.1 (C-12′), 127.8 (C-14′), 127.5 (C-15′), 99.3 (C-1), 74.2 (C-3), 72.1 (C-2), 70.0 (C-4), 69.7 (C-5), 63.2 (C-6), 55.4 (OCH$_3$, C-7), 33.5, 31.5, 29.3, 27.2, 26.5, 3 × 25.6, 24.7, 22.5 (10 × aliphatic **C**H$_2$, C2′–C4′, C7′, C10′, C13′, & C16′–C19′), 14.0 (terminal aliphatic **C**H$_3$, C-20′) ppm. HRMS (ESI-MS) *m*/*z* calc. for C$_{27}$H$_{44}$O$_7$, [M + H]$^+$ 481.3160, found 481.3157.

Methyl 6-*O*-9-decenoyl-β-D-glucopyranoside (4b)

White solid (72 mg, 80% yield). Melting point (DSC): 85.5 °C. ^{1}H NMR (400 MHz, CDCl$_3$): δ 5.80 (m, 1H, CH$_2$C**H**=CH$_2$, H-9′), 4.96 (m, 2H, CH$_2$CH=C**H**$_2$, H-10′), 4.51 (dd, $J_{6a,6b;6a,5}$ = 12.3, 4.5 Hz, 1H, C**H**$_2$OCO, H$_a$-6), 4.28 (dd, $J_{6b,6a;6b,5}$ = 12.2, 2.1 Hz, 1H, C**H**$_2$OCO, H$_b$-6), 4.20 (d, $J_{1,2}$ = 7.7 Hz, 1H, C**H**OCH$_3$, H-1), 3.57 (m, 4H, overlapping signals, C**H**OH, H-3 & OC**H**$_3$, H-7), 3.45 (m, 1H, C**H**OH, H-5), 3.36 (m, 2H, overlapping signals, 2×C**H**OH, H-2 & H-4), 2.36 (t, $J_{2',3'}$ = 7.6 Hz, 2H, C**H**$_2$CO, H-2′), 2.03 (m, 2H, C**H**$_2$CH=CH$_2$, H-8′), 1.61 (m, 2H, CH$_2$C**H**$_2$CH$_2$, H-3′), 1.29 (m, 8H, 4×C**H**$_2$, H4′–H7′) ppm. ^{13}C NMR (101 MHz, CDCl$_3$): δ 175.0 (**C**=O, C-1′), 139.2 (**C**H=CH$_2$, C-9′), 114.3 (CH=**C**H$_2$, C-10′), 103.7 (C-1), 75.9 (C-3), 74.2 (C-5), 73.7, 69.9 (C-2,4), 63.1 (C-6), 57.4 (OCH$_3$, C-7), 34.2 (C-2′), 33.8 (C-8′), 29.2, 29.1, 29.0, 28.9 (4 × aliphatic **C**H$_2$, C4′–C7′), 25.0 (C-3′) ppm. HRMS (ESI-MS) *m*/*z* calc. for C$_{17}$H$_{30}$O$_7$, [M + H]$^+$ 347.2064, found 347.2067.

Methyl 6-*O*-10-undecenoyl-β-D-glucopyranoside (4d)

White viscous solid (64 mg, 69% yield). Melting point (DSC): 92.6 °C. ^{1}H NMR (400 MHz, CDCl$_3$): δ 5.80 (m, 1H, CH$_2$C**H**=CH$_2$, H-10′), 4.95 (m, 2H, CH$_2$CH=C**H**$_2$, H-11′), 4.41 (dd, $J_{6a,6b;6a,5}$ = 12.2, 5.2 Hz, 1H, C**H**$_2$OCO, H$_a$-6), 4.32 (dd, $J_{6b,6a;6b,5}$ = 12.1, 1.9 Hz, 1H, C**H**$_2$OCO, H$_b$-6), 4.20 (d, $J_{1,2}$ = 7.7 Hz, 1H, C**H**OCH$_3$, H-1), 3.55 (m, 4H, overlapping signals, C**H**OH, H-3 & OC**H**$_3$, H-7), 3.46 (m, 1H, C**H**OH, H-5), 3.36 (m, 2H, overlapping signals, 2×C**H**OH, H-2 & H-4), 2.35 (t, $J_{2',3'}$ = 7.6 Hz, 2H, C**H**$_2$CO, H-2′), 2.02 (m, 2H, C**H**$_2$CH=CH$_2$, H-9′), 1.60 (m, 2H, CH$_2$C**H**$_2$-CH$_2$, H-3′), 1.28 (m, 10H, 5×C**H**$_2$, H4′–H8′) ppm. ^{13}C NMR (101 MHz, CDCl$_3$): δ 174.8 (**C**=O, C-1′), 139.3 (**C**H=CH$_2$, C-10′), 114.3 (CH=**C**H$_2$, C-11′), 103.7 (C-1), 76.0 (C-3), 74.1 (C-5), 73.6, 70.1 (C-2,4), 63.3 (C-6), 57.3 (OCH$_3$, C-7), 34.2 (C-2′), 33.9 (C-9′), 29.4, 29.3, 2 × 29.2, 29.0 (5 × aliphatic **C**H$_2$, C4′–C8′), 25.0 (C-3′) ppm. HRMS (ESI-MS) *m*/*z* calc. for C$_{18}$H$_{32}$O$_7$, [M + H]$^+$ 361.2221, found 361.2222.

Methyl 6-*O*-(9E)-octadecenoyl-β-D-glucopyranoside (4f)

White solid (71 mg, 60% yield). Melting point (DSC): 75.0 °C. ^{1}H NMR (400 MHz, CDCl$_3$): δ 5.37 (m, 2H, CH$_2$C**H**=C**H**CH$_2$, H-9′,10′), 4.46 (dd, $J_{6a,6b;6a,5}$ = 12.1, 4.8 Hz, 1H, C**H**$_2$OCO, H$_a$-6), 4.30 (dd, $J_{6b,6a;6b,5}$ = 12.2, 2.0 Hz, 1H, C**H**$_2$OCO, H$_b$-6), 4.20 (d, $J_{1,2}$ = 7.8 Hz, 1H, C**H**OCH$_3$, H-1), 3.56 (m, 4H, overlapping signals, C**H**OH, H-3 & OC**H**$_3$, H-7), 3.45 (m, 1H, C**H**OH, H-5), 3.36 (m, 2H, overlapping signals, 2×C**H**OH, H-2 & H-4), 2.36 (t, $J_{2',3'}$ = 7.6 Hz, 2H, C**H**$_2$CO, H-2′), 1.94 (m, 4H, C**H**$_2$CH=CHC**H**$_2$, H-8′,11′), 1.60 (m, 2H, CH$_2$C**H**$_2$CH$_2$, H-3′), 1.25 (m, 20H, 10×C**H**$_2$, H4′–H7′ + H12′–H17′), 0.87 (t, $J_{18',17'}$ = 6.8 Hz, 3H, CH$_2$C**H**$_3$, H-18′) ppm. ^{13}C NMR (101 MHz, CDCl$_3$): δ 174.9 (**C**=O, C-1′), 130.6 (CH=**C**H, C-9′), 130.3 (**C**H=CH, C-10′), 103.7 (C-1), 75.9 (C-3), 74.2 (C-5), 73.7, 70.0 (C-2,4), 63.1 (C-6), 57.3 (OCH$_3$, C-7), 34.2, 32.7, 32.6, 32.0, 2 × 29.7, 29.6, 29.4, 29.3, 2 × 29.2, 29.1, 25.0, 22.8 (14 × aliphatic **C**H$_2$, C2′–C8′ & C11′–C17′), 14.2 (terminal aliphatic **C**H$_3$, C-18′) ppm. HRMS (ESI-MS) *m*/*z* calc. for C$_{25}$H$_{46}$O$_7$, [M + H]$^+$ 459.3316, found 459.3320.

Methyl 6-*O*-(5Z,8Z,11Z,14Z)-eicosatetraenoyl-β-D-glucopyranoside (4i)

Transparent viscous liquid (71 mg, 57% yield). ^{1}H NMR (400 MHz, CDCl$_3$): δ 5.36 (m, 8H, (CH$_2$C**H**=C**H**CH$_2$)$_4$, H-5′,6′,8′,9′,11′,12′,14′,15′), 4.46 (dd, $J_{6a,6b;6a,5}$ = 12.1, 4.8 Hz, 1H, C**H**$_2$OCO, H$_a$-6), 4.31 (dd, $J_{6b,6a;6b,5}$ = 12.3, 1.9 Hz, 1H, C**H**$_2$OCO, H$_b$-6), 4.20 (d, $J_{1,2}$ = 7.8 Hz, 1H, C**H**OCH$_3$, H-1), 3.56 (m, 4H, overlapping signals, C**H**OH, H-3 & OC**H**$_3$, H-7), 3.46 (m, 1H, C**H**OH, H-5), 3.36 (m, 2H, overlapping signals, 2×C**H**OH, H-2 & H-4), 2.82 (m, 6H, (CH=CHC**H**$_2$)$_3$CH=CH, H-7′,10′,13′), 2.38 (t, $J_{2',3'}$ = 7.7 Hz, 2H, C**H**$_2$CO, H-2′), 2.08 (m, 4H, C**H**$_2$(CH=CHCH2)$_3$CH=CHC**H**$_2$, H-4′,16′), 1.71 (m, 2H, CH$_2$C**H**$_2$CH$_2$, H-3′), 1.32 (m, 6H, 3×C**H**$_2$, H-17′,18′,19′), 0.88 (t, $J_{20',19'}$ = 6.9 Hz, 3H, CH$_2$C**H**$_3$, H-20′) ppm. ^{13}C NMR (101 MHz, CDCl$_3$): δ 174.4 (**C**=O, C-1′), 130.6 (C-5′), 129.0 (C-6′), 128.9 (C-8′), 128.7 (C-9′), 128.4 (C-11′), 128.2 (C-12′), 127.9 (C-14′), 127.6 (C-15′), 103.6 (C-1), 76.1 (C-3), 74.0 (C-5), 73.5, 70.2 (C-2,4), 63.5 (C-6), 57.3 (OCH$_3$, C-7), 33.6, 31.6, 29.4, 27.3, 26.6, 3 × 25.7, 24.9, 22.6 (10 × aliphatic **C**H$_2$, C2′–C4′, C7′, C10′, C13′, & C16′–C19′), 14.2 (terminal aliphatic **C**H$_3$, C-20′) ppm. HRMS (ESI-MS) *m*/*z* calc. for C$_{27}$H$_{44}$O$_7$, [M + H]$^+$ 481.3160, found 481.3164.

Bacterial strain and growth conditions

The Gram-positive bacterial strain *Staphylococcus aureus* ATCC 25923 was employed as the model organism to evaluate the antibacterial efficacy of the synthesized CFAE derivatives. The strain was routinely cultured on Plate Count Agar (PCA) and preserved at 4 °C for short-term storage. For experimental procedures, a single colony from the PCA plate was aseptically transferred into 10 mL of Tryptic Soy Broth (TSB) and incubated at 37 °C for 18 h to obtain the working culture. The resulting bacterial suspension was standardized to an optical density equivalent to a 0.5 McFarland standard (approximately 1.5 × 10^8 CFU mL^{-1}), measured using a Densimat photometer (BioMerieux, France). Subsequently, the culture was diluted with sterile TSB to yield a final inoculum concentration of 1 × 10^6 CFU mL^{-1} for use in antibacterial assays.

Preparation of CFAE solutions for assay

Lauric acid (**2a**) and oleic acid (**2e**), each with a purity of approximately 99%, along with vancomycin hydrochloride

derived from *Streptomyces orientalis* (≥900 μg mg^{-1} as vancomycin base), were procured from Sigma-Aldrich and employed as reference standards for comparative evaluation of the synthesized CFAE derivatives. Stock solutions of all tested CFAE, including both the novel compounds and reference standards, were prepared at a concentration of 10 mM using a sterile hydroalcoholic solvent system composed of ethanol and deionized water in a 1 : 1 ratio. These stock solutions were aliquoted and stored at −20 °C until further use. Prior to antibacterial testing, working solutions were prepared by diluting the stock preparations in Tryptic Soy Broth (TSB) to a final concentration of 1 mM.

Assessing the antibacterial activity of CFAE

The antibacterial properties of the synthesized CFAE were evaluated against the selected microbial strain utilizing a standardized microtiter plate-based assay, adapted from the methodology outlined by Jaiswal *et al.*[69,70] In brief, serial dilutions of each tested compound were prepared aseptically in sterile Tryptic Soy Broth (TSB), with triplicates dispensed into 96-well microtiter plates (Sarstedt Ltd) to a final volume of 100 μL per well. Subsequently, 100 μL of the standardized bacterial suspension (1×10^6 CFU mL^{-1}) was added to each well, yielding a total volume of 200 μL per well. Blank wells, also in triplicate, consisted of 100 μL of each diluted compound mixed with 100 μL of sterile TSB, without bacterial inoculum. Control groups encompassed: (i) wells containing only sterile TSB (200 μL) to account for media background; (ii) wells with bacteria and TSB alone (100 μL each), serving as bacterial growth controls; and (iii) wells containing 100 μL of bacterial inoculum and 100 μL of 10% v/v ethanol in TSB, resulting in a final ethanol concentration of 5% v/v, to evaluate any potential antimicrobial contribution from the solvent used in compound preparation.

All plate setups were prepared in duplicate and incubated for 24 h at 37 °C using a Powerwave Microplate Spectrophotometer (BioTek, USA), with optical density (OD_{600}) readings recorded at hourly intervals under continuous, low intensity shaking in kinetic mode. Upon completion of the incubation, aliquots from each well were streaked onto Plate Count Agar (PCA) to determine bacterial viability. The minimum inhibitory concentration (MIC) was defined as the lowest concentration of the tested compound that visibly suppressed microbial growth following 24 h of incubation at 37 °C. The minimum bactericidal concentration (MBC) corresponded to the lowest concentration at which no bacterial growth was observed upon subculturing onto agar media. Additionally, the percentage of inhibition was determined using the following eqn (2):

$$\% \text{ Inhibition} = \frac{\text{Control value} - \text{Sample value}}{\text{Control value}} \times 100 \quad (2)$$

The combination of OD measurements and post-incubation plate cultures was used to calculate percentage of inhibition, minimum inhibitory concentration (MIC), and minimum bactericidal concentration (MBC).

Results and discussion

Screening of "greener" solvents in CFAE synthesis and determination of optimal solvent

A preliminary qualitative solubility screen of MAG (**1a**) in *t*-BuOH, a solvent previously reported for CFAE synthesis,[1–3,21,50] was undertaken by dissolving 50 mg of MAG (0.26 mmol) in varying solvent volumes (0.5–5 mL, corresponding to 515–51.5 mM) to assess the effect of concentration and temperature on solubility. Complete dissolution was observed at ≤85.83 mM of MAG and 60 °C for an observed period of 5 h (SI, Fig. S1). This informed the completion of a series of parallel esterification reactions of MAG (**1a**, 1 equiv.) and LA (**2a**, 2 equiv.) in both *t*-BuOH and MeCN in the same set of reactions (515–51.5 mM of MAG) at 60 °C for 48 h, to assess solubility impact within reaction mixtures, with yields quantified by ^{1}H qNMR as outlined in the experimental. In both solvents, 85.83 mM of MAG yielded optimal monoester production at this scale. Reactions in MeCN (72%) provided more than two-fold yield compared to *t*-BuOH (32%) at this concentration (SI, Table S1).

We evaluated several further solvents based on chosen solvent characteristics from established solvent selection guides, including CHEM21, in reactions performed at a fixed MAG concentration of 85.83 mM (3 mL reaction volume).[71] Solvents that have previously been employed in CFAE production, including acetone and *t*-BuOH, are classified as recommended solvents by CHEM21 due to their safety profiles, biodegradability, and low toxicity. The polar aprotic solvents applied in CFAE synthesis *i.e.*, MeCN and DMSO are categorized as problematic solvents (by CHEM21 ranking after discussion) due to challenges in managing large-scale waste treatment, environmental persistence, and high boiling temperature (DMSO).[71] Although the CHEM21 solvent selection guide integrates and compares multiple solvent assessments from industry, in the updated 2015 version of the GSK solvent sustainability guide, MeCN was reclassified from the red to amber category, recognizing it as a less problematic solvent.[72] In our reactions, MeCN was selected based on this classification, and its literature-supported effectiveness in CFAE synthesis with other derivatives.[21,24]

The solvent investigation was extended, to include potentially eco-friendlier substitutes. These solvents included 2-methyltetrahydrofuran (2-MeTHF), dimethyl isosorbide (DMI), cyclopentyl methyl ether (CPME), diethyl carbonate (DEC), limonene, γ-valerolactone (GVL), propylene carbonate (PC), ethylene carbonate (EC) and dihydrolevoglucosenone (Cyrene™) (Scheme 1).

The solvents acetone, *t*-BuOH, and MeCN, supported generation of yields of 26, 40 and 73% of MAG monolaurate **3a**, respectively (Table 1, Entries 7, 8, and 5). The potentially bio-derived solvents CPME and 2-MeTHF provided product in yields of 9 and 18% (Table 1, Entries 11 and 10). Limonene did not facilitate any reaction which was confirmed by analyzing TLC of the reaction crude (Table 1, Entry 12). The TLC analysis of reaction completed in Cyrene™ (boiling point 227 °C) was ineffective, as analytes were covered by a dominating solvent

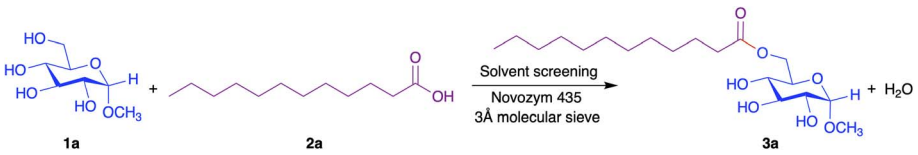

1a 2a 3a

Scheme 1 Synthesis of methyl 6-*O*-dodecanoyl-α-D-glucopyranoside **3a** using 1 : 2 equiv. of MAG (**1a**, 0.26 mmol): LA (**2a**), 50 and 80 wt% CALB and molecular sieves w.r.t MAG, heated at 60 °C and stirred at 100 rpm for 48 h, assessed in various solvents. The product yield was obtained by ^{1}H qNMR on the dried reaction crude.

Table 1 Yield of MAG monolaurate **3a** from reactions completed in a series of solvents, as determined by ^{1}H qNMR from reaction crudes

Entry	Solvent	CAS no.	Normalized Reichardt's parameter (E_T^N)	log *P*	Yield of **3a** (%)
1	EC	96-49-1	0.552 (ref. 77 and 78)	−0.90 (ref. 79)[a]	56[b]
2	Cyrene™	53716-82-8	0.333 (ref. 80)	−0.71 (ref. 79)[a]	No reaction[c]
3	DMI	5306-85-4	—	−0.44 (ref. 81)	Trace[d]
4	PC	108-32-7	0.472 (ref. 77 and 82)	−0.41 (ref. 79)[a]	59[e,f]
5	MeCN	75-05-8	0.460 (ref. 36 and 82)	−0.33 (ref. 83)	73[f]
6	GVL	108-29-2	0.301 (ref. 36 and 84)	−0.27 (ref. 79)[a]	52[e,f]
7	Acetone	67-64-1	0.355 (ref. 77 and 82)	−0.23 (ref. 83)	26[f,g]
8	*t*-BuOH	75-65-0	0.389 (ref. 77 and 82)	0.35 (ref. 29 and 85)	40[f]
9	DEC	105-58-8	0.185 (ref. 77 and 82)	1.21 (ref. 85)	Impurity formation[d]
10	2-MeTHF	96-47-9	0.187 (ref. 84)	1.85 (ref. 85)	18[f]
11	CPME	5614-37-9	—	1.59 (ref. 39)	9[f]
12	Limonene	138-86-3	0.046 (ref. 84)	4.80 (ref. 86)	No reaction[d]

[a] Where experimental log *P* values were not available, values were obtained from ChemSpider, which reports predicted log *P* values generated using the ACD/Labs Percepta Kernel – PhysChem Module version: 14.[79] [b] Isolated yield after chromatography. [c] Reaction crude was analyzed by TLC and ^{1}H NMR. [d] Reaction crudes were analyzed by TLC. [e] GVL and PC were removed by silica gel flushing followed by ^{1}H qNMR analysis for yield determination and this step did not constitute purification or removal of unreacted LA. [f] Reaction crudes were analyzed by ^{1}H qNMR (Method A – CD_3OD and fumaric acid as internal standard).[53] [g] The reaction was performed at 50 °C.

spot (Table 1, Entry 2). Subsequent ^{1}H NMR analysis of the reaction crude confirmed no product formation. The reaction in DMI resulted in trace monoester **3a** by TLC (Table 1, Entry 3). A trace of unwanted product was obtained in reactions completed in DEC by TLC, where a faint spot appeared which did not match the MAG monolaurate **3a** spot (Table 1, Entry 9). This may arise from a transesterification (transcarbonation) reaction involving the carbonate solvent (DEC) with the carbohydrate substrate (MAG), as dimethyl carbonate (DMC) has been reported to undergo Novozym 435 catalyzed transesterification with soybean oil,[73] while it also reacts with glycerol *via* transcarbonation to form glycerol carbonate.[74] However, this was not confirmed in our work.

Finally, the screening of GVL, PC, and EC provided positive results by TLC. Due to the high boiling point of GLV (207 °C), PC (242 °C) and EC (248 °C, solid at 20 °C) effectively prohibiting rotary evaporation, these solvents were removed through a silica plug from their respective reaction crude (8 : 2 solvent gradient of *n*-heptane : EtOAc, followed by 100% MeOH to obtain the concentrated reaction crude). The silica gel flush was performed solely for solvent removal and did not result in purification of the reaction mixture. Subsequently, ^{1}H qNMR analysis of the solid crude revealed yields of 52% and 59% for MAG monolaurate **3a** for reactions completed in GVL and PC, respectively (Table 1, Entries 6 and 4).

Removal of solvent was difficult with EC, as this solidified on the silica bed. Therefore, the product was isolated by flash column chromatography (9 : 1 solvent gradient of *n*-heptane : EtOAc to 5 : 5 *n*-heptane : EtOAc), affording a 56% yield of **3a** (Table 1, Entry 1). To consider these solvents as greener alternatives, the associated work-up must be clearly included. Alternative work-ups have been reported, for example liquid–liquid extraction using immiscible organic solvent systems such as PC with *n*-hexane[75] or diisopropyl ether (DIPE)[48] to recover non-polar products. In our reactions, these solvents applied in extraction were unsuccessful, requiring silica gel flush to remove solvent and obtain the solid crude mixture.

From all reactions and respective solvents assessed, MeCN proved to be the most efficient in the screening, with 73% yield of CFAE (obtained by ^{1}H qNMR). The non-classical solvents, PC and EC could also be seen as effective alternative solvents for CFAE synthesis. From these, PC is the best alternative solvent, supporting the highest yield. It can also be noted that this solvent can use CO_2 in its preparation, in an atom economic manner,[76] and with its Hansen solubility parameters (HSP) close to MeCN suggests comparable solvating ability (SI, Table S2).[36] It offers potential be a sustainable alternative to MeCN, with an appropriate work-up. Given that GVL was noted as not included by Jordan *et al.* in their reported condensed replacement polar aprotic solvent selection guide, due to concerns for its sedative properties,[36] potential for abuse, and possible future legislative restriction, the reaction was not progressed for further assessment in this solvent.

Correlation between physicochemical properties of solvents and yield

Solvent hydrophobicity, specifically log *P* (octanol/water partition coefficient), is frequently used to explain solvent effects in lipase-catalyzed CFAE synthesis. Here, the reaction medium must support both a hydrophilic carbohydrate substrate and a hydrophobic fatty acid while preserving the essential hydration microenvironment of an immobilized enzyme.[4,23,29,50,87] In this context, solvents with very low log *P* (such as DMSO: −1.3)[50] values are often associated with reduced activity due to disruption of the enzyme hydration layer, whereas highly non-polar (log *P* > 4) solvents may limit carbohydrate solubility and reduce reaction rates. Consequently, intermediate log *P* ranges are often reported as favorable.[4,23,50]

In addition to log *P*, empirical solvent polarity scales such as normalized Reichardt's parameter (E_T^N) have been used to correlate solvent polarity with CFAE reaction outcomes. For example, Fischer *et al.* correlated conversion with E_T^N of solvents for lipase-catalyzed maltose linoleate synthesis and reported that solvents with intermediate polarity were generally more effective than those of very low (*n*-hexane/toluene; E_T^N: 0.01–0.1) or high polarity (DMSO; E_T^N: 0.45).[23] However, both log *P* and solvent polarity (E_T^N) are indicative but not predictive, as exceptions such as DMSO, DMF, dioxane, and *t*-BuOH may reflect additional factors, particularly specific solvent–enzyme interactions, that influence the reaction outcome.[23,50]

In our study, both parameters were examined (Table 1). Highly non-polar limonene (very high log *P*: 4.80; very low E_T^N: 0.046) afforded no detectable product, consistent with insufficient carbohydrate solubilization. However, the behaviour of polar/low log *P* solvents did not appear to be uniform: EC and PC gave moderate yields (56% and 59%; Table 1, Entries 1 and 4), whereas Cyrene™ and DMI gave no or only trace of product, respectively, despite having a broadly similar low log *P* (−0.41 to −0.90) and polarity region (Table 1, Entries 1–4).

Neither log *P* alone nor E_T^N showed a strictly linear correlation with yield. For example, MeCN ($\log P = -0.33$; $E_T^N = 0.460$) afforded the highest yield of 73%, GVL ($\log P = -0.27$; $E_T^N = 0.301$) gave a moderate yield (52%), whereas acetone ($\log P = -0.23$; $E_T^N = 0.355$) afforded substantially lower yield (26%) under our conditions. Likewise, *t*-BuOH ($\log P = 0.35$; $E_T^N = 0.389$) deviated from a simple monotonic trend with 40% yield. These exceptions confirm that the correlations based solely on log *P*/E_T^N can be less effective, as solvent specific interactions with the enzyme and substrates may also govern reaction performance including hydrogen-bonding, dipolarity/polarizability, and effects on enzyme hydration.[4,23,50]

Accordingly, solvent effects were analyzed using Kamlet–Taft parameters (π*, α, β), which incorporates "polarity" into dipolarity/polarizability (π)* and hydrogen-bond donor/acceptor characteristics (α/β). Here, the hydrogen-bond acceptor capacity of solvent *i.e.*, basicity (β) can compete for interactions in the catalytic microenvironment, which may influence esterification efficiency and selectivity. Therefore, Kamlet–Taft analysis was applied to provide a further mechanistically informative basis for solvent selection in CFAE synthesis. To our knowledge, the influence of the solvent physicochemical properties by applying Kamlet–Taft (KT) parameters, on the yield and selectivity of the reaction has not been undertaken (solvents with their KT values are provided in Table S2, SI).[88] Therefore, KT solvent parameters of basicity (β) and polarity/polarizability (π*) were compared and analyzed graphically, against yield obtained (Fig. 2). The correlation plot indicated that solvents with high polarity (π* > 0.70) and low to moderate basicity (β ∼0.30–0.60) may potentially achieve reaction yield >50%, with MeCN, PC, EC, and GVL falling within this region. However, this can only be stated tentatively as there are several exceptions. For example, with a similar β value and higher π* value of EC (π*, β; 0.99, 0.32) compared to MeCN (π*, β; 0.75,0.31), higher yield could be expected. However, a combination of possible decreased activity of Novozym 435 in the more polar EC and difficulties with purification using column chromatography could lead to a lower yield in this instance. Despite acetone having favourable KT parameters (π*, β; 0.71, 0.48), the yield (26%) was likely impacted by conducting the reaction at 50 °C, due to its boiling point (56 °C). Literature has reported the successful Novozym 435-catalyzed CFAE synthesis in acetone at *ca.* 45–65 °C,[23,27,50,87,89–92] including MAG (**1a**) and LA (**2a**) esterification at 60 °C to form the monoester **3a**.[52] Thus, the lower yield in acetone likely results from both solvent effects and the lower reaction temperature used, rather than only an unfavourable KT profile. A further exception is *t*-BuOH (π*, β; 0.41, 0.93), which provided monoester (**3a**) in 40% yield, despite having much higher β, and lower π* than the solvents outlined above. This outcome could be influenced by the higher hydrogen-bonding ability of *t*-BuOH with the substrates. The yield obtained with CMPE may also point to this possibility by comparison (π*, β; 0.42, 0.53, yield 9%). Using 2-MeTHF (π*, β; 0.53, 0.58), the yield doubled to 18%, with higher polarity and comparable basicity to CPME, improving carbohydrate solubility.

In reactions applying limonene, DEC, DMI, and Cyrene™ as solvents, a trace or no product was formed. Here the impact is less clear, with possible solubility, or competing reactions impacting reaction rate.[93,94]

For further development, MeCN was identified as the most effective solvent with respect to yield and isolation, with potential for innovation in its manufacture from biomass[95] and bioethanol to avoid supply problems.[96] In addition, a study has reported MeCN as a greener and less hazardous solvent for Steglich esterification, substituting hazardous chlorinated or amide solvents.[97]

Optimization of reaction parameters and scale-up of reaction

Effect of reaction time on the yield of monoester product (3a). Published optimal reaction times for CALB (Novozym 435) catalyzed esterification of MAG with fatty acids tends to be variable. For example, Mutschler *et al.* reported reaction times of 1–3 days for equimolar mixture of MAG and fatty acids ($C_{10:0}$ – $C_{16:0}$ saturated FAs and oleic acid; $C_{18:1}$) using an incubation and shaking approach at 60–80 °C, with HPLC-determined MAG conversion of 43–88%, depending on the fatty acids and

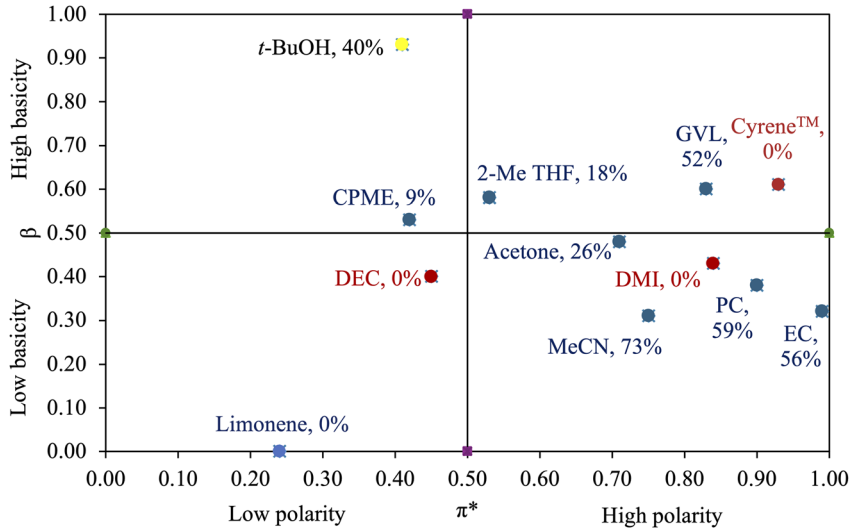

Fig. 2 Correlation of Kamleft Taft (KT) solvent parameters *i.e.*, polarity (π*) and basicity (*β*) evaluating their influence on yield of **3a**.

solvent.[52] A maximum MAG conversion of 62% was reported for lauric acid ($C_{12:0}$) in dioxane at 60 °C.[52] In dual-solvent system of 1-hexyl-3-methylimidazolium trifluoromethylsulfonate and 2-methyl-2-butanol ([HMIm][TfO] (IL)/2M2B: 0.05 : 0.95, v/v), Zhao *et al.* reported a 24 h incubation period at 45 °C for equimolar mixture of methyl glucoside and lauric acid, achieving ~70% methyl glucoside conversion, calculated as ester product formed relative to the total methyl glucoside initially added.[49] Using 1 : 3 equiv. of MAG : LA, Gelo-Pujic *et al.* reported 55% conversion of MAG applying conventional oil-bath heating compared to 95% conversion under microwave heating at 95 °C for 5 h, with product formation analyzed by GC and HPLC.[64]

In our study, the reaction time optimization was conducted for the model esterification reaction in MeCN using conventional oil-bath heating, with ^{1}H qNMR yields determined on the dried reaction crudes.[53] From a series of reactions, it was observed that by increasing the reaction time from 2 to 4 to 8 h, the yield of monoester (**3a**) increased from 49.58% to 74.22% to 82.29%, respectively (Table 2, Entries 1–3). For the 2 h reaction, two equally intense anomeric proton signals of product and MAG substrate at *δ* 4.61 and 4.64 ppm, respectively, indicated approximately equal proportions of unreacted substrate and product. Beyond 2 h, the signal of MAG was further reduced, indicating increased substrate consumption and higher product formation (SI, Fig. S2). The yield showed minimal change (82.29–81.71%) when the reaction time was increased from 8 to 24 h in 4 h intervals and in fact reduced when extended to 72 h in 24 h intervals (from 81.71 to 73.89%; Table 2, Entries 7–9) (Fig. 3). The formation of di-ester and other impurities was noted in reactions above 8 h. This was evident by the appearance in the ^{1}H NMR the C-6 proton signal assigned to that of a di-ester at *δ* 4.14 ppm (confirmed by ^{1}H NMR of isolated di-substituted product) and other impurity signals at *δ* 4.58 ppm (SI, Fig. S3). This suggested that prolonged reaction time could lead to lower product yield, purity, and regioselectivity. A reaction time of 4 h was therefore established as the standard for further optimization studies, a shorter reaction time relative to previous reports for CALB-catalyzed MAG esterification with LA (which ranged from 5 to 72 h).[49,52,64] Subsequent optimization of other reaction parameters further improved the monoester (**3a**) yield to 89.82% within 4 h, as presented below.

Effect of reaction temperature, molecular sieve loading, molar ratio, and catalyst loading on product (3a) yield. Reaction temperature plays a crucial role, influencing substrate solubility and enzyme activity in lipase-catalyzed CFAE synthesis.[3] To assess its impact on the model reaction completed in MeCN, four distinct temperature points were evaluated at 40 °C, 50 °C, 60 °C, and 70 °C in 4 h reactions (Table 2, Entries 10–13). The product yield increased with temperature from 40 °C (49.90%) to 50 °C (62.40%), reaching a maximum of 74.22% at 60 °C, analyzed by ^{1}H qNMR (Table 2, Entries 10–12). A slight drop to 72.32% yield at 70 °C was observed, therefore temperature was maintained at 60 °C (Table 2, Entry 13). Interestingly, di-esters were not formed at this elevated temperature in 4 h. The reduced signal intensity of MAG **1a** at *δ* 3.5, 3.8, and 4.64 ppm, along with increased anomeric proton signals of product at *δ* 4.61 ppm in the ^{1}H NMR analysis confirmed the trend when increasing from 40 to 60 °C (SI, Fig. S4). These results indicate that 60 °C provides favorable conditions for substrate (MAG) solubility, generating higher product yield, as determined by ^{1}H NMR. This finding aligns with literature reports suggesting the suitable temperature range of 40–60 °C for Novozym 435 in CFAE synthesis, where moderate heating helps overcome mass-transfer limitations of highly polar carbohydrate substrates, while maintaining enzyme activity.[3,4,29,52]

In lipase-catalyzed CFAE synthesis applying esterification, efficient water removal is necessary to shift the equilibrium toward ester production, while preserving enough hydration to sustain enzyme activity.[4,29] In reports, molecular sieves (MS) were found to be most efficient as the water adsorbent relative

Table 2 Summary of the CALB catalyzed synthesis of MAG monoester **3a**: the impact of reaction time, temperature, molecular sieve loading, MAG : LA molar ratio, and catalyst loading on product yield as determined by ^{1}H qNMR[a,c]

Entry	Time (h)	Temperature (°C)	Novozym 435 – wt% of **1a**	3 Å MS – wt% of **1a**	Molar ratio MAG : LA	Mean ^{1}H qNMR yield ± SD ($n = 2$)[b] (%)
1	2	60	50	80	1 : 2	49.58 ± 0.70
2	4					74.22 ± 1.36
3	8					82.29 ± 3.46
4	12					82.80 ± 0.78
5	16					82.17 ± 2.38
6	20					79.18 ± 2.67
7	24					81.71 ± 0.38
8	48					78.27 ± 1.79
9	72					73.89 ± 1.85
10	4	40		80	1 : 2	49.90 ± 1.15
11		50				62.40 ± 1.70
12		60				74.22 ± 1.36
13		70				72.32 ± 1.24
14	4	60		50	1 : 2	72.72 ± 0.14
15				80		75.33 ± 2.93
16				150		74.20 ± 2.91
17				200		76.54 ± 1.56
18	4	60		80	1 : 1	49.10 ± 1.82
19					1 : 2	74.30 ± 2.30
20					1 : 3	87.36 ± 0.51
21					1 : 4	86.33 ± 0.21
22	4	60	25	80	1 : 3	48.24 ± 0.22
23			50			89.82 ± 1.35
24			75			90.89 ± 1.21

[a] All reactions were performed using 1 equiv. MAG (**1a**, 0.26 mmol, 85.83 mM) in 3 mL MeCN and stirred at 100 rpm in an oil-bath, heated by a stirrer hotplate. [b] ^{1}H qNMR yield data are presented as mean values ± standard deviations (SD) ($n = 2$) as completed on dry reaction crude. All means and standard deviations are rounded to two decimal places; $n = 2$: reactions were performed and crudes analyzed in duplicate by ^{1}H qNMR Method A.[53] [c] Individual replicate yield data are given in the SI for each tested parameter.

to $CaCl_2$, $CaSO_4$, and $MgSO_4$ in sugar ester production.[98] In our studies, thermally activated 3 Å MS were tested at 50, 80, 150 and 200 wt% loading to MAG (**1a**). The yield of MAG monolaurate (**3a**) slightly increased from 72.72 to 75.33% with an increase from 50 to 80% loading of MS (Table 2, Entries 14 and 15). However, increasing the loading further to 150 and 200 wt% diminished the improvement (Table 2, Entries 16 and 17). No clear difference in the anomeric signal intensity of product (**3a**) and MAG (**1a**) was observed across the four tested MS loading experiments by ^{1}H qNMR analysis (SI, Fig. S5).

In CFAE esterification reactions, a molar excess of fatty acid is preferable to shift the equilibrium towards ester formation.[3] However, excess substrate can alter the polarity of the reaction medium, affecting solubility and enzyme accessibility.[29]

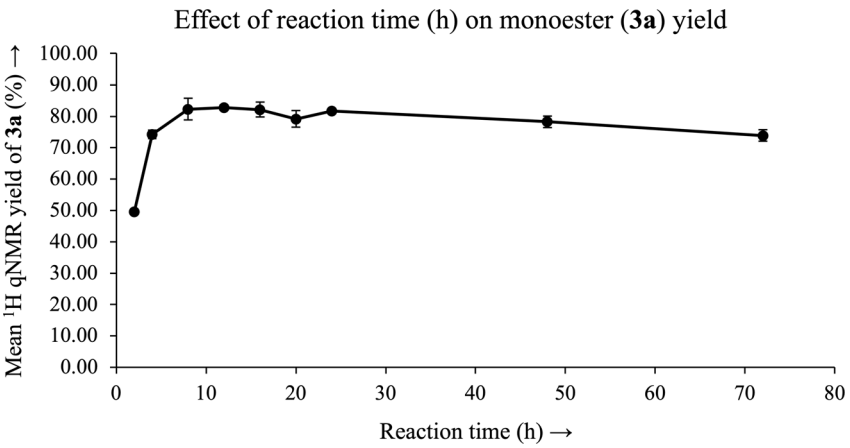

Fig. 3 Yield of **3a** over time determined by ^{1}H qNMR analysis of the dried crude for reactions performed in duplicate (1 : 2 equiv. of **1a** (0.26 mmol, 85.83 mM): **2a**, 50 and 80 wt% CALB and 3 Å MS of **1a**, respectively) using 3 mL MeCN at 60 °C and 100 rpm in oil-bath heating setup; included error bars are based on standard deviations ($n = 2$).

Mutschler *et al.* reported maximum MAG conversions of 62% for 1 : 1 molar ratio of MAG (**1a**) to LA (**2a**) in dioxane, under incubation heating conditions (product yields were not reported).[52] For a 1 : 3 molar ratio of **1a** : **2a**, Gelo-Pujic *et al.* reported 55% MAG conversion in diethyl ether with oil-bath heating.[64] For the 1 : 3 molar ratio of **1a** to **2a**, Ariffin *et al.* reported an isolation strategy for the product (**3a**) and its characterization. However, no information on substrate conversion or product yield was provided.[51] In our study, four different molar ratios of MAG (**1a**) to LA (**2a**), 1 : 1, 1 : 2, 1 : 3, and 1 : 4 were evaluated using the previously optimized reaction parameters (Table 2, Entries 18–21), with 1 : 3 molar ratio observed as optimal (87.36% ^{1}H qNMR yield). The anomeric proton signals of MAG at δ 4.64 ppm gradually decreased in reactions performed with 1 : 1 to 1 : 3 molar ratio of MAG : LA, indicating increased consumption of MAG and higher product formation with increasing equivalents of LA (SI, Fig. S6).

Finally, the catalyst loading was examined with the goal of minimizing the catalyst input. Gelo-Pujic *et al.* reported the use of 1 g of Novozym 435 for 1–1.5 mmol of MAG (**1a**), corresponding to ~350–520 wt% catalyst relative to the substrate (**1a**). Mutschler *et al.* reported a 50 wt% loading of Novozym 435 relative to **1a** in assessment of organic solvent. In comparison, our study evaluated enzyme loadings of 25, 50 and 75 wt% relative to **1a**. The ^{1}H qNMR yield of MAG monolaurate (**3a**) increased from 48.24 to 89.82%, when Novozym 435 loading was raised from 25 to 50 wt%, which is consistent with the optimal 50 wt% catalyst loading reported by Mutschler *et al.* for 1 : 1 molar ratio of MAG : LA (Table 2, Entries 22 and 23).[52] However, further increasing the loading to 75 wt% did not result in a sufficient improvement in the product yield to justify the extra added enzyme quantity (90.89%; Table 2, Entry 24). The overall loading trend can be visualized by the anomeric signal of both product (**3a**) and MAG (**1a**), where the anomeric signal of substrate (MAG, **1a**) at δ 4.64 ppm reduced markedly from 25 to 50 wt% loading, with no further reduction at 75 wt%. (SI Fig. S7).

Overall, the optimization experiments were performed in duplicate ($n = 2$) to allow practical assessment of multiple reaction variables, including solvent, reaction time, temperature, molecular sieve loading, MAG : LA molar ratio, and catalyst loading. We acknowledge that $n = 2$ limits formal statistical comparison between closely performing conditions. Therefore, while choosing the final reaction conditions, slight numerical variations were carefully analyzed. As discussed, the selections were based not only on the highest numerical yield, but also on process-relevant considerations. For instance, in the temperature investigation, 60 °C produced the highest yield, which is consistent with reported suitable conditions for Novozym 435. Similarly, 80 wt% 3 Å molecular sieves provided comparable yield to higher loadings while avoiding excessive drying of the reaction system and unnecessary solid input. A MAG : LA molar ratio of 1 : 3 maximized product yield without the additional excess fatty acid required at 1 : 4. For catalyst loading, 50 wt% Novozym 435 was selected because increasing the loading to 75 wt% gave only a marginal yield improvement, which did not justify the additional enzyme input. Together, these decisions provided a high-yielding and practically balanced set of conditions, by eliminating additional increases in temperature, drying agent, fatty acid, or enzyme loading when no appreciable increase in yield was observed.

Recycling study of Novozym 435. Enzyme recovery, recycling, and operational stability are crucial for maximizing utilization, reducing material consumption, and improving sustainability of biocatalysed processes, further broadening their industrial applications.[28,99,100] In our process, the immobilized CALB (Novozym 435) was evaluated for recyclability. This was initially assessed over three successive reactions performed with 1 : 2 molar ratio of MAG : LA. Initially, two reaction conditions were assessed. In the first approach, physically recovered Novozym 435 beads were directly reused in subsequent reaction cycles. In the second approach, the recovered CALB beads were dried in a vacuum desiccator prior to reuse. In both cases, additional fresh sieves were added for each cycle and the previously used sieves physically removed. In this work, the fresh CALB provided 69.11% yield of CFAE, followed by 68.25 and 66.02% for the first and second reuse of undried CALB, respectively. This indicated that CALB retained activity over three reactions (Table 3, Recycled CALB, Entries 1–3, 1 : 2 molar ratio of MAG : LA). In contrast, the vacuum dried recovered CALB resulted in a drastic decrease in yield from 69.93 to 9.33% over three reactions (Table 3, Recycled CALB dried under vacuum, Entries 1–3) (Fig. 4). Drying the CALB (Novozym 435 beads) may have resulted in loss of activity by removing water from the enzyme, required for its stability and catalytic activity.[29,98,101] The yield loss trend is supported by ^{1}H qNMR spectra (SI; Table S8 and Fig. S8). Therefore, direct reuse of Novozym 435 offers a practical strategy to improve process sustainability by reducing catalyst consumption.

It should be noted that the yield obtained with fresh CALB in this recycling study which employed a 1 : 2 molar ratio of MAG to LA, (which was not fully optimized) (69.11% and 69.93%; Table 3, Entry 1) was slightly lower than that observed during optimization experiments (74.22%, 74.22%, and 75.33%; Table 2, Entries 2, 12, and 15). Across five independent experiments conducted on different days under the identical conditions of MAG : LA 1 : 2 molar ratio, the relative standard deviation (RSD) of ^{1}H qNMR yield was calculated to be 3.90% using eqn (1). This is below the recommended 5% threshold used to indicate good precision in analytical measurements,[53,102,103] indicating good experimental repeatability of the reaction under the tested conditions. The observed variation of yield between optimization and recycling studies may arise from differences in commercially obtained Novozym 435 batches or bead size distribution, both of which can influence catalytic activity.

To assess further MAG : LA molar ratio, recyclability, and long-term operational stability, the enzyme recyclability was further investigated under the fully optimized reaction conditions (1 : 3 molar ratio of MAG : LA) for seven reaction cycles over a period of 10 days. A gradual decrease in the ^{1}H qNMR yield of product (**3a**) was observed from 89.82% to 67.13% across the seven cycles, corresponding to an overall reduction of 22.69% yield by the seventh cycle (Fig. 4). The detailed ^{1}H qNMR

Table 3 Yield of product **3a** in the enzyme recycling study determined by ^{1}H qNMR[a]

Entry	Reaction cycle	Mean ^{1}H qNMR yield ($n = 2$) using recycled CALB (%), (MAG : LA – 1 : 2 equiv.)[b]	Mean ^{1}H qNMR ($n = 2$) using recycled CALB dried under vacuum (%), (MAG : LA – 1 : 2 equiv.)[b]	Mean ^{1}H qNMR yield ($n = 2$) using recycled CALB under optimized condition (%), (MAG : LA – 1 : 3 equiv.)[c]
1	1st reaction	69.11 ± 0.52	69.93 ± 0.96	89.82 ± 1.35
2	2nd reaction	68.25 ± 0.31	25.78 ± 1.15	81.49 ± 0.36
3	3rd reaction	66.02 ± 0.32	9.33 ± 1.51	77.37 ± 0.24
4	4th reaction	—	—	73.19 ± 0.36
5	5th reaction	—	—	73.78 ± 0.22
6	6th reaction	—	—	69.95 ± 0.38
7	7th reaction	—	—	67.13 ± 0.56

[a] Reactions were completed in duplicate ($n = 2$) and analyzed in duplicate by ^{1}H qNMR of dried crude, using published Method A.[53] ^{1}H qNMR yield data are presented as mean values ± standard deviations ($n = 2$); values are rounded to two decimal places. Individual replicate yield data and corresponding NMR spectra are given in the SI (Table S8, S9 and Fig. S8, S9). Freshly activated 3 Å MS were added for each reaction cycle in all cases. [b] Reactions were carried out with 1 : 2 molar ratio of MAG (**1a**, 50 mg/0.26 mmol, 85.83 mM) : LA (**2a**), Novozym 435–50 wt% of **1a**, 3 Å MS – 80 wt% of **1a**, in 3 mL of MeCN at 60 °C and 100 rpm on a hotplate stirrer with an oil-bath. [c] Reactions were performed under optimized conditions using 1 : 3 molar ratio of MAG : LA, with all other parameters unchanged.

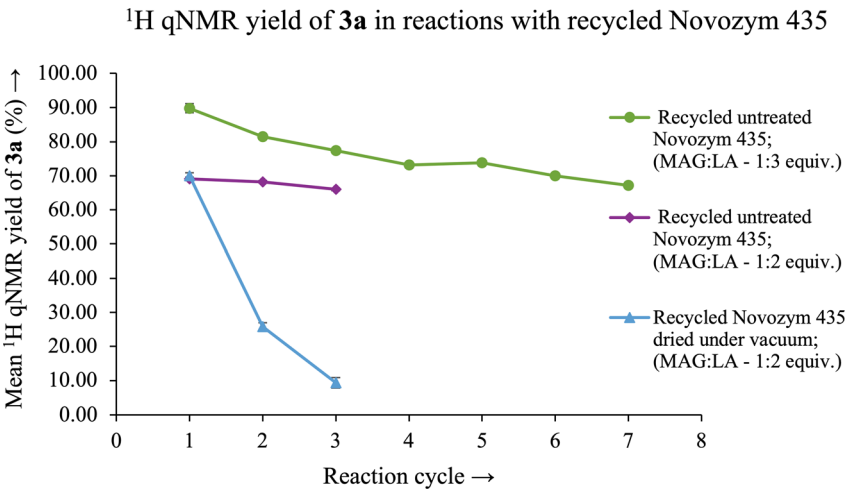

Fig. 4 Graph showing the trend in ^{1}H qNMR yield of **3a** in the CALB (Novozym 435) recycling study under the optimized conditions of 1 : 3 molar ratio of MAG (**1a**) : LA (**2a**) for seven successive 4 h reaction batches (Novozym 435 untreated, green line) and pre-optimized conditions of 1 : 2 molar ratio of **1a** : **2a** for three successive 4 h reaction batches (Novozym 435 untreated, purple line and Novozym 435 vacuum dried, blue line); error bars included based on standard deviations ($n = 2$).

yield data, calculated from the crudes, and representative spectra are provided in the SI (Table S9 and Fig. S9).

Previous studies have reported progressive loss of Novozym 435 activity upon reuse. For example, in the esterification of methyl α-D-glucopyranoside (MAG, **1a**) and oleic acid, Akoh and Mutua *et al.* reported a total drop of 33.6% in the oleic acid incorporation (from 71.9% to 38.3%) by the eighth reaction cycle using immobilized lipase SP382 in benzene/pyridine (molar ratio of 2 : 1). This was attributed to the incomplete removal of residues from the biocatalyst between cycles, hindering substrate and enzyme contact.[99] Vescovi *et al.* reported a 31% decrease in fructose conversion for fructose oleate synthesis after nine 6 h batches using Novozym 435 in *t*-BuOH at 55 °C.[104] The activity loss was attributed to a combination of thermal inactivation, enzyme leaching from the non-covalently bound support, the presence of water in the esterification reaction, and incomplete removal of compounds adsorbed to the Novozym 435 bead surface between reaction cycles.[104] D. An *et al.* also investigated the recycling of enzyme across six consecutive reactions for the esterification of D-glucose with *N*-capryl glycine (1 : 1.5 molar ratio) at 55 °C with a reaction time of 9 h, where the Novozym 435 beads were recovered using *n*-hexane and vacuum-dried for 24 h prior to reuse.[28] Under these conditions, the yield of 6-*O*-(*N*-capryl glycine)-glucopyranose decreased gradually from ~72% to ~42%, corresponding to an overall yield reduction of 30% over six reactions. In comparison, our study showed a gradual yield decline of 22.69% over seven reactions under optimized conditions without vacuum drying (Fig. 4). However, vacuum drying of Novozym 435 after reaction led to a substantial loss of activity, with a total ~60% decrease in yield observed over three successive reactions (Table 3, Recycled CALB (dried under vacuum), Entries 1–3), highlighting how CALB performance is sensitive to drying and

post-reaction handling procedures, which may also be specific to the substrates and the reaction.

Several factors have been reported to contribute to the deactivation of Novozym 435 upon reuse.[100] The use of reaction medium in organic solvent such as MeCN may lead to the partial dissolution of immobilized support of Novozym 435.[100] Another limitation of the polymeric beads of Novozym 435 (Lewatit) under magnetic stirring is mechanical fragility,[100,105,106] although in this study, this was prevented by careful control of stirring conditions (at 100 rpm) to avoid bead fracture. In the CFAE esterification process, the hydrophilic carbohydrate substrate (MAG) and water as a by-product may accumulate within the moderately hydrophilic support of Novozym 435, potentially hindering mass transfer and contributing to gradual catalytic deactivation.[100] Enzyme leaching from the non-covalent immobilization of CALB on Lewatit VP OC 1600 could occur at elevated temperature of 60 °C.[100] Additionally, enzyme may release from the support in the presence of detergent-like species.[100,107] Considering the amphiphilic nature of methyl glucoside fatty acid ester (hydrophilic carbohydrate head and hydrophobic fatty acid tail), the monoester product (**3a**) may contribute to partial CALB desorption from Novozym 435 beads during recycling. These combined effects could contribute to the gradual decrease in catalytic activity observed across the Novozym 435 recycling reactions in the present study. These were not probed experimentally during this work.

Recovery of unreacted lauric acid (LA) and green chemistry metric evaluation for the gram-scale synthesis of 3a: EcoScale and Chem21 first-pass toolkit. The optimised reaction and non-chromatographic work up were successfully scaled to 1.17 g input of carbohydrate (**1a**), yielding 1.89 g of monoester (**3a**) in 83.50% isolated yield, as shown in Scheme 2.

Our molar ratio optimization study showed that increasing the equivalents of LA (**1a** : **2a** – 1 : 3 equiv.) improved the yield of monoester product **3a** (Table 2, Entries 18–21). However, this also results in an increase in material intake, which may compromise green chemistry metrics, particularly lowering the reaction mass efficiency (RME). Therefore, recovery of this excess was undertaken for reuse in a potentially circular manner. In the gram-scale synthesis of product (**3a**), the reaction crude was subjected to non-chromatographic purification (EtOAc : H_2O workup followed by trituration with *n*-heptane) to precipitate monoester product (**3a**). Evaporation of the *n*-heptane filtrate under reduced pressure afforded 2.50 g of unreacted LA, corresponding to 69.30% recovery relative to the total 3.61 g input of LA. The recovered LA exhibited 99.69% purity as determined by ^{1}H qNMR (refer to SI, Section 13) and this was characterized by ^{1}H NMR (SI, Fig. S13). This recovered material can therefore potentially be reused in subsequent reactions, reducing waste and improving RME. For the gram-scale synthesis of product (**3a**), the initial RME was 39.53%. Following the recovery of unreacted LA, the adjusted RME was calculated to be 83.19%, highlighting more than a two-fold improvement in the RME (refer to assessment of CHEM21 first-pass toolkit and Section 11 in the SI for calculation of RME).

The gram-scale synthesis of **3a**, from reaction to product isolation, was assessed using two established green metric evaluation tools: EcoScale[57] and CHEM21 first-pass toolkit.[108]

EcoScale has been widely used to evaluate synthetic organic protocols by penalising reaction parameters that adversely affect the process efficiency.[57] However, its use alongside additional green metrics is recommended to be more effective, as EcoScale scoring alone may overlook important parameters when comparing different synthetic protocols.[109,110] Mass-based green metrics such as Process Mass Intensity (PMI) and E-factor provide insight into factors contributing to waste and their improvements. The CHEM21 first-pass toolkit was therefore also evaluated which incorporates Atom Economy (AE), RME, PMI, and additional sustainability parameters.[108]

Evaluation of the EcoScale score. The EcoScale score of the optimized gram-scale synthesis of **3a** was evaluated to be 75.75 (Table 4), classifying the protocol as an excellent procedure based on EcoScale criteria.[57] Compared to previous studies,[52,64] the high isolated yield of **3a** (83.50%), efficient purification without column chromatography, use of a conventional stirrer/oil-bath heating setup instead of a shaker, the recovery of excess unreacted LA, and reuse of biocatalyst contributed to this score. The pricing component did not include Novozym 435 as a consumable reagent, as its reuse was demonstrated without experiencing a substantial loss of catalytic activity. This approach is consistent with literature evaluating the EcoScale score in which Novozym 435 (biocatalyst) was not penalized in the pricing component due to its demonstrated recovery and reuse.[57,109,110] EcoScale cost estimates (Table 4, Parameter 2) are based on a normalised 10 mmol product basis, generated from gram-scale experimental data in this study (5 mmol of isolated product). As defined by the EcoScale methodology, only reaction components are considered in the cost evaluation (Table 4).[57] Industrial amortisation and comprehensive downstream isolation costs, which would eventually decide the final cost of the product, are not included in this assessment and should be considered as a limitation of our study. We clearly acknowledge that our reaction is completed at bench scale and such analyses would be required for potential translation of the proposed

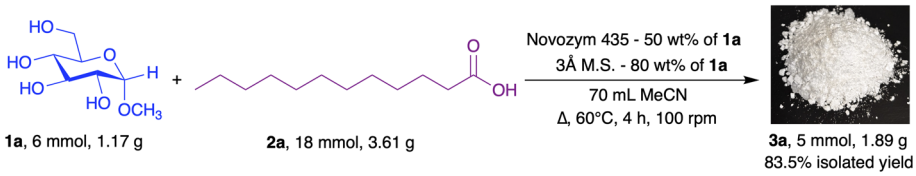

Scheme 2 Gram-scale reaction to isolate product **3a**.

Table 4 EcoScale evaluation for the optimized synthesis of **3a**. EcoScale score = (100 − Σindividual penalties), >75 – excellent; >50 – acceptable; and <50 – inadequate[a]

Parameter	Penalty points description	Penalty points
1 Yield	(100 − % isolated yield)/2 = (100 − 83.50)/2 = 8.25	8.25
2 Price of reaction components (to obtain 10 mmol of product)	(MAG + LA + 3 Å MS + MeCN) = €3.91/$ 4.55 for 10 mmol product (SI, Table S10 for calculation). Determined as inexpensive (<$10) = 0	0
3 Safety[b]	MeCN: (T) toxic + (F) highly flammable = 5 + 5	10
4 Technical setup	Common setup (stirrer/oil-bath and standard glassware)	0
5 Temperature/time	Heating > 1 h (60 °C for 4 h) = 3	3
6 Work up/purification	Liquid–liquid extraction (EtOAc: H_2O followed by *n*-heptane wash) = 3	3
Total penalties	—	24.25
EcoScale score	=(100–24.25)	75.75

[a] EcoScale score is >75 which suggests an excellent synthesis protocol. [b] In EcoScale evaluation only reaction solvent *i.e.*, MeCN is considered. For safety and sustainability aspects of reaction and workup purification, all solvents were assessed by CHEM21 first-pass tool kit.

process further through scale up to pilot-scale synthesis and commercial manufacturing.

Assessment with the CHEM21 first-pass toolkit. The CHEM21 first-pass toolkit was applied to evaluate the performance of the process at the discovery stage and identify areas for improvement.[108] This framework assesses promising reactions using key green chemistry indicators including yield, AE, RME, PMI, solvent assessment, catalyst use, critical elements in terms of their long term availability, energy requirements, batch or flow processing, work-up considerations, health and safety aspects based on Hazard (H)-statements and Substances of Very High Concern (SVHC), commercial availability of chemicals, and reaction applicability through substrate scope, thereby providing a structured evaluation of the process.[108] Together, these parameters inform the material efficiency, environmental impact, and practical applicability of proposed synthetic protocol. In this study, all CHEM21 first-pass parameters were assessed for the gram-scale synthesis **3a**. For complete assessment including mass-based metrics calculations, refer to SI (Section S11 and provided excel file). As noted by Monteith,[111] PMI at discovery stage can present limitations due to the small scale of experiments. While more comprehensive metrics, such as renewable intensity (RI) and life-cycle assessment (LCA), are typically applied at later stages within CHEM21 second (2–10 L scale in batch) and third-pass evaluations,[108] a screening LCA was included to provide an initial assessment of environmental impacts at the bench scale.

All mass inputs from reaction to product isolation (1 : 3 molar ratio of MAG : LA; 1.17 g/6.03 mmol: 3.61 g/18.02 mmol yielded 1.89 g of isolated **3a**, 83.50% yield) are listed in SI (Table S11). For the green metric calculations including PMI, masses of all materials used in the process were included, including molecular sieves, Novozym 435 (considered at end-of-life, despite partial recyclability), Na_2SO_4, and filter paper. In this work, molecular sieves were not recycled and conservatively classified as waste in the PMI calculations (gram-scale synthesis of **3a**).

The atom economy and carbon economy were 95.43% and 100%, respectively, indicating high regioselectivity with only H_2O as by-product. From an initial 3.61 g of LA input, the recovery of 2.50 g of unreacted LA (69.30%) improved material efficiency. Accounting for this recovered LA, the adjusted RME and Optimum Efficiency (OE) improved to 83.19% from 39.53% and 87.17% from 41.40%, respectively (SI, Section S11). The total PMI (142.73 g g^{-1}) from reaction to product isolation was divided into two main components *i.e.*, $PMI_{reaction}$ = 32.51 g g^{-1} and PMI_{workup} = 110.22 g g^{-1}. $PMI_{reaction}$ was further subdivided into $PMI_{reactants,reagents,and\ catalyst}$ = 3.33 g g^{-1} and $PMI_{reaction\ solvent(s)}$ = 29.17 g g^{-1} and PMI_{workup} to $PMI_{workup\ chemicals}$ = 6.89 g g^{-1} and $PMI_{workup\ solvents}$ = 103.33 g g^{-1}, respectively (SI, Section S11). This indicates that the solvent use ($PMI_{reaction\ solvent(s)+workup\ solvents}$ = 132.50 g g^{-1}; 92.83%) dominated the total PMI, highlighting solvent management as the principal area for improvement. Future PMI reduction should therefore prioritize lowering work-up solvent quantities, focusing on recovery and reuse of EtOAc and *n*-heptane, reducing or replacing *n*-heptane in the trituration step, and minimizing reaction solvent use where substrate solubility allows. During further process development and scale-up, improved phase separation, crystallization techniques, solvent recycling, and potential transition to continuous-flow processing could further reduce solvent intensity and improve overall process mass efficiency.

Previous studies on MAG (**1a**) esterification with LA (**2a**) vary in the level of process detail reported, which can limit the calculation of mass-based metrics, particularly RME and PMI.[49,51,52,64] In our work, the mass inputs for reaction, work-up generating reaction crude, and workup-based product isolation steps were systematically documented, enabling quantitative sustainability assessment using EcoScale and the CHEM21 first-pass toolkit. This provides a benchmark dataset that allows for direct comparison of green chemistry metrics for future CFAE synthetic protocols.

In contrast to the transesterification route which requires preparation of vinyl esters of fatty acids as starting materials, this esterification strategy reduces additional reagents and by-

products.[1] However, the CHEM21 solvent assessment identifies MeCN and *n*-heptane as problematic, where EtOAc, H_2O, and MeOH are classified as preferred solvents. This remains a limitation of the current process. Future solvent substitution should therefore focus on replacing MeCN with suitable greener polar aprotic alternatives. In this study, PC gave the most promising yield among the non-classical solvents screened. However, its high boiling point (242 °C) and associated work-up challenges currently limit its direct replacement of MeCN. Further development should therefore prioritize improved work-up or solvent recovery strategies for PC-based reactions, together with reduction, recovery, or replacement of *n*-heptane in the product isolation step. Among the materials used, MeOH (H370) and *n*-heptane (H400, H410) possess health and safety concerns with red-flagged H-codes (refer to excel file in SI for details).[71] MeOH was used to recover unreacted MAG for ^{1}H qNMR analysis, however, aqueous extraction removes unreacted MAG from the organic phase (EtOAc), indicating that MeOH can be avoided for direct product isolation post reaction.

The Novozym 435 was reused across seven cycles with a 22.69% decrease in yield by the seventh reaction, reducing catalyst consumption and improving the environmental profile compared to chemical catalysis. Both carbohydrate (MAG, **1a** and MBG, **1b**) and fatty acids can be derived from renewable resources such as potato starch and plant oils,[52] respectively, and are commercially available at >100 g scale from multiple suppliers (*e.g.*, Merck and Fluorochem). The reaction was conducted using a standard laboratory heating setup at 60 °C, below the boiling point of MeCN (82 °C), with a measured energy consumption of 0.207 kWh under optimized conditions (60 °C, 4 h, and 100 rpm). The gram-scale synthesis of **3a** demonstrates laboratory-scale applicability of the optimized method and provides a basis for sustainability assessment. However, it should not be interpreted as direct evidence of industrial-scale implementation. Although the work-up based purification replaces column chromatography, it substantially adds to PMI through solvent use (H_2O, EtOAc, and *n*-heptane) and therefore remains an important target for future process optimization through solvent reduction, recovery, or transition to flow-based processing. The substrate scope with 18 CFAE (16 isolated, 2 isolated with impurities) from two carbohydrate substrates (MAG and MBG) and 9 fatty acids demonstrates the applicability of the synthetic method. It must be noted that disappointingly the purification of liquid CFAE products required preparative-TLC, limiting larger-scale applicability for liquid-based CFAE.

Overall, the CHEM21 evaluation highlights both sustainability advantages, such as renewable inputs, catalyst reuse, substrate recovery, and efficient product (**3a**) isolation and remaining challenges, such as solvent intensity and workup limitation for purification of liquid CFAE products associated with the present synthetic process.

Life cycle analysis (LCA): cradle-to-gate screening assessment for gram-scale synthesis of 3a. To provide a broader evaluation of the environmental effects of the gram-scale synthesis of MAG monolaurate (**3a**), a screening cradle-to-gate LCA was carried out. LCA complements green chemistry metrics by accounting for material inputs, energy consumption, waste treatment, and related environmental and health-related impacts across a defined system boundary.[58,59] However, applying LCA at laboratory scale remains challenging as the evaluation needs comprehensive life cycle inventory data, which can be difficult to obtain for small-scale and developing synthetic protocols.[58,112] In this screening LCA, a detailed precursor-based inventory reconstruction, such as that reported by Mathew *et al.*,[59] was not performed. Proxy data were used where exact raw material data were unavailable in Ecoinvent database and this represents a limitation of the current LCA. Therefore, the absolute impact values should be considered informative rather than definitive. Nonetheless, the approach remains appropriate for early process development to identify environmental hotspots and relative trade-offs and demonstrates how LCA may be considered and applied in the research laboratory.

Environmental impacts were assessed using the ReCiPe 2016 endpoint method. As detailed by Mathew *et al.*, in the ReCiPe 2016 methodology, the midpoint indicators, including global warming, water consumption, fossil resource scarcity, and ozone depletion, are aggregated into three endpoint damage indicators: human health, ecosystem quality, and resource scarcity.[59] These three endpoint indicators are normalized and weighted to provide a single score result expressed in points.[59] The contribution analysis based on individual material and energy inputs identified electricity consumption as the dominant environmental hotspot, accounting for 40.77 milli points (mPt) of the endpoint single score impact (Fig. 5). This was followed by hazardous waste incineration (8.83 mPt), solvents such as EtOAc (6.97 mPt) and MeCN (6.38 mPt), while other inputs, including sodium sulfate, enzyme production, and molecular sieve proxy materials, contributed comparatively less. This was further supported by midpoint characterization, where electricity contributed most strongly across multiple midpoint categories such as, global warming, ionizing radiation, fossil resource scarcity, and human toxicity (SI, Fig. S10). The overall endpoint score was dominated by the human health category, as the weighting factors in the ReCiPe method are determined by policy and monetisation targets, where stakeholders and policymakers are expected to invest in preventing damage to human health compared to ecosystem and resource scarcity.

The dominance of electricity is primarily associated with activation of 3 Å molecular sieves. Although this step is not directly related to the chemical transformation, its activation required 4.475 kWh, which is ~91% of the total measured electricity consumption for the complete synthesis of **3a** (4.903 kWh; SI, Table S14). A comparative analysis of processes with and without electricity for activation of 3 Å MS showed a substantial reduction in environmental impact when this energy input was excluded (Fig. 6). Under this scenario, the total impact of the complete process decreased from 65.65 mPt (Fig. 6A) to 28.44 mPt (Fig. 6B), while the reaction stage decreased from 48.34 mPt to 11.13 mPt, and the purification stage remain unchanged at 17.31 mPt as this stage did not include 3 Å MS activation. This emphasizes the importance of accounting for auxiliary energy requirements in laboratory scale

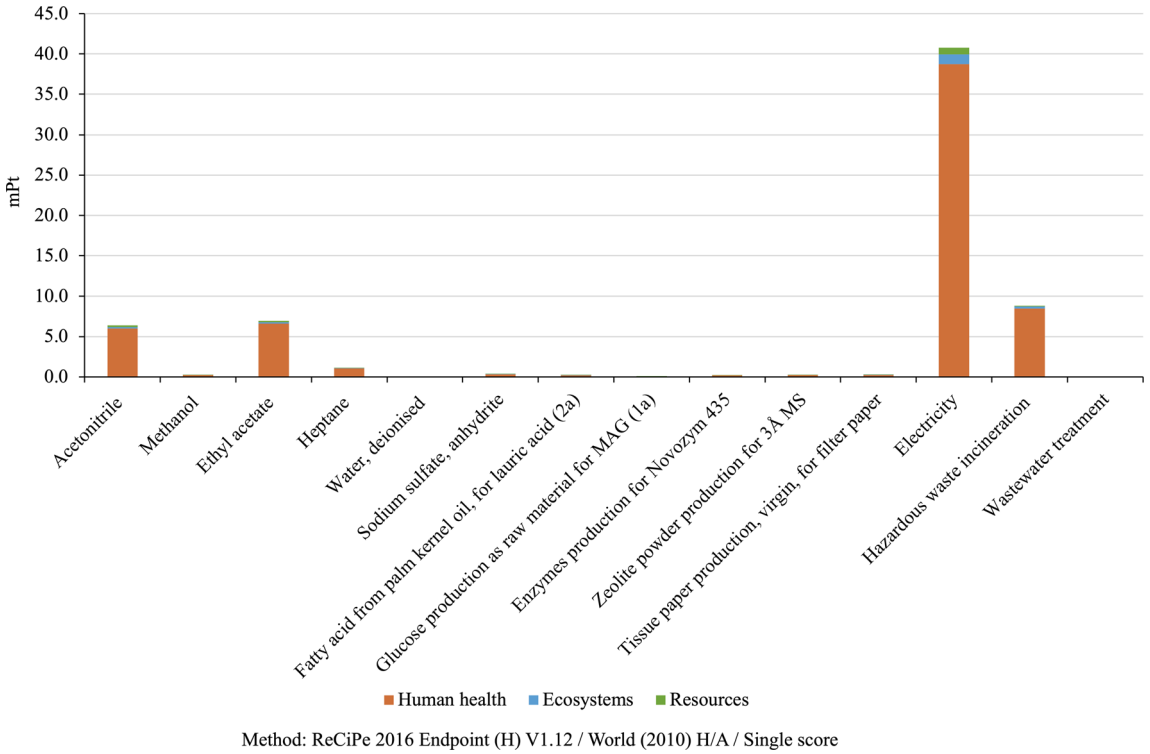

Fig. 5 Single score (mPt) contribution of individual material and energy inputs to the end point impact indicators (human health, ecosystems, and resources) of the complete synthesis of 1 g MAG monolaurate (**3a**), calculated using SimaPro® 10.3.0.3.

synthesis, where such steps can outweigh the impacts of material inputs in LCA.

As described in the methodology and SI LCI, this LCA was designed as a screening cradle-to-gate assessment using gram-scale foreground inventory data and proxy datasets where exact inventory data were unavailable. Therefore, uncertainty is associated with these proxy dataset selections, and the results should be interpreted as indicative hotspot-identification data rather than a full comparative or industrial-scale environmental assessment. It must be noted that when compared to optimized larger-scale operations, where equipment utilization, batch size, and process integration are more efficient, laboratory-scale systems may overestimate energy use and related environmental implications.[59,112,113] This current screening LCA is based on gram-scale experimental data (functional unit: 1 g of **3a**), where resource utilization is not at full capacity and therefore represents a limitation. Overall, these findings represent a key opportunity to improve the environmental performance of the synthesis of **3a**, by optimizing the energy intensive auxiliary steps and solvent usage.

Substrate scope expansion with unsaturated fatty acids. As discussed, the initial phase of this work optimised the model enzyme catalysed esterification of LA (**2a**, saturated fatty acid) with MAG (**1a**). LA (**2a**) afforded monoesters **3a** and **4a** in 84% and 79% isolated yields within 4 h, respectively. A. Smith *et al.* reported the chemical catalyzed synthesis of **3a** and **4a** in 86% and 75% isolated yields after 24 h, respectively, with products isolated by column chromatography.[6] Gelo-Pujic *et al.* reported CALB catalyzed synthesis of **3a**, with only HPLC derived conversions of 55% and 95% for MAG (**1a**) under conventional and microwave heating conditions, respectively.[64] Applying 4 h reaction time, the substrate scope was explored using a panel of unsaturated fatty acids (uFAs, **2b–i**) using methyl α/β-D-glucopyranosides (**1a** and **1b**) to assess reaction generality and antimicrobial activity. Monoesters derived from these uFAs afforded 55–84% isolated yields for both **1a** and **1b**, except for the α,β-unsaturated fatty acid **2c**, which gave <10% yield of products **3c** and **4c**.

Our reaction conditions were applied effectively, however modifications in the work up phase were required, particularly for monoesters derived from liquid fatty acids. With medium chain monounsaturated fatty acids (MC-MUFAs, **2b–d**), the C-6 monoesters of 9-decenoic acid (**2b**, C10 : 1, terminal alkene), **3b** and **4b** were obtained in 84% and 80% isolated yield, respectively (Scheme 3). In switching to higher chain MUFAs (C11 : 1, **2c** and **2d**; structural isomers), the reaction of 2-undecenoic acid (α,β-unsaturated, **2c**) with **1a** and **1b** was much less efficient, affording <10% yield for both **3c** and **4c**, with impurities present. The reduced reactivity of **2c** could be explained by the lower esterification efficiency of the conjugated α,β-unsaturated carbonyl carbon with decreased electrophilicity and limited rotational freedom between the α- and carbonyl carbon in **2c**, compared to unconjugated analogues such as **2d**.[114,115] The reaction of **1a** and **1b** with 10-undecenoic acid (terminal alkene, **2d**) resulted in yields of 64 and 69% for **3d** and **4d**, respectively. The decreased yield for both **1a** and **1b** with **2d** (C11 : 1, terminal alkene) compared to **2b** (C10 : 1, terminal alkene) may be due to additional carbon chain, reducing ability to interact with the

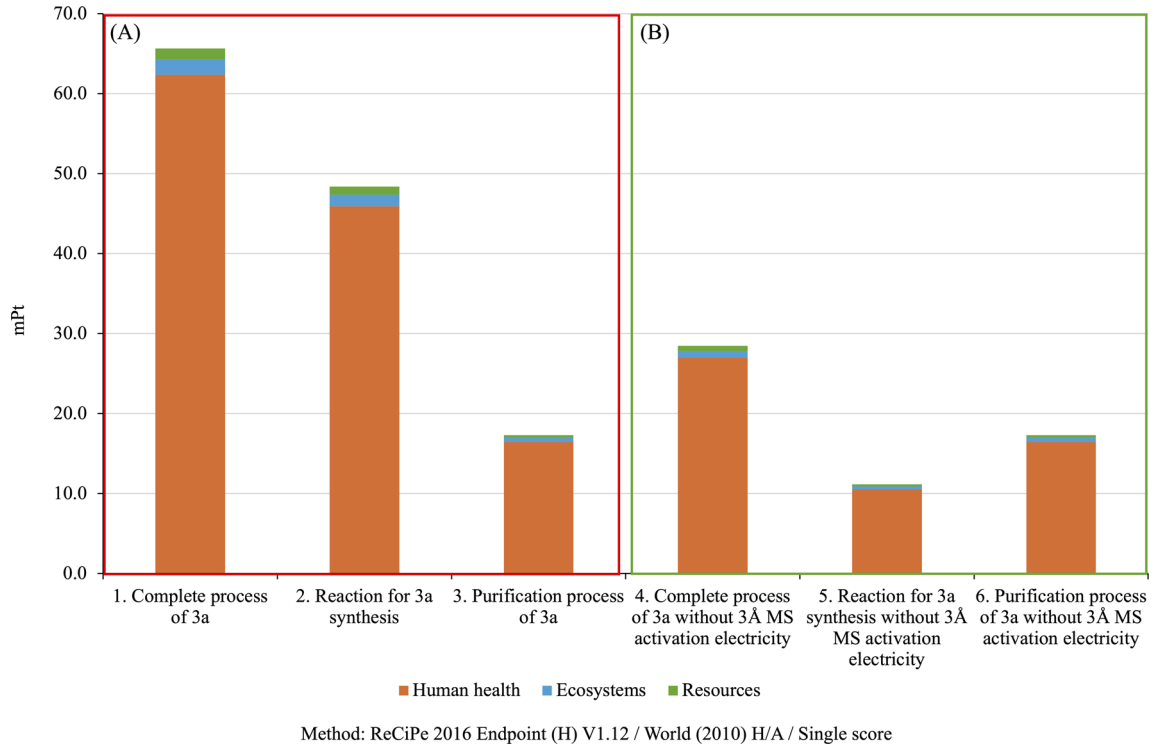

Fig. 6 Comparison of end point single scores (mPt) for the synthesis of 1 g **3a**, including complete process, reaction step, and purification step; (A): base model including electricity for 3 Å molecular sieve activation and (B): without this electricity input, calculated using SimaPro® 10.3.0.3.

CALB catalytic triad or could be minor solubility differences affecting enzyme accessibility.

The synthesis of esters of long chain unsaturated fatty acids was also investigated. Two geometrical isomers and ω-9 based long chain monounsaturated fatty acids (LC-MUFAs), oleic acid (**2e**, *cis*) and elaidic acid (**2f**, *trans*) yielded isolated C-6 monoesters in 57% (**3e**) and 64% (**3f**) with MAG (**1a**), and 59% (**4e**) and 60% (**4f**) with MBG (**1b**), respectively. No significant yield difference was observed between the *cis* and *trans* isomers, possibly due to the presence of the double bond at the C-9 position which may reflect equal rates of binding of these substrates within the CALB active site. In comparison, Mutschler *et al.* reported a maximum 50% conversion of MAG (**1a**) for the CALB-catalysed esterification of **1a** with oleic acid (**2e**), using an ionic-liquid coated enzyme system, where isolated or analytical product yields were not reported.[52] The long chain polyunsaturated fatty acids (LC-PUFAs), ω-6 linoleic acid (**2g**, $C_{18:2}$), ω-3 linolenic acid (**2h**, $C_{18:3}$) and ω-4 arachidonic acid (**2i**, $C_{20:4}$) were evaluated in the esterification process. Isolated yields of 55–61% were obtained for **3g**, **3h**, **4g** and **4h** for C_{18} based **2g** and **2h** (Scheme 3). Switching to arachidonic acid (**2i**, $C_{20:4}$), the isolated yield was 57% for both **3i** and **4i**. Hence, within the LC-PUFAs (C_{18}–C_{20}), *cis* isomers which were assessed, variations in the degree of unsaturation and double-bond position had only a modest effect on esterification efficiency, suggesting that the fatty acid chain primarily influences substrate solubility and enzyme accessibility.

For purification of the synthesized compounds, monoesters derived from saturated, terminal alkene, and *trans* isomer based fatty acids, such as **3a**, **3b**, **3f**, **4a**, **4b** and **4f** were successfully isolated using an extractive work up EtOAc : H_2O followed by *n*-heptane wash to remove unreacted fatty acid. These monoesters being solids, were insoluble in *n*-heptane, enabling efficient separation of the unreacted fatty acid and isolation of the product as a white precipitate. In contrast, the monoesters derived from unsaturated fatty acids (uFAs) including **2e**, **2g**, **2h** and **2i** (**3e**, **3g**, **3h**, **3i**, **4e**, **4g**, **4h** and **4i**) were obtained as viscous liquids, while the products **3d** and **4d** from uFA **2d** were obtained as white viscous solid. All these monoesters remained soluble in *n*-heptane, preventing effective separation of the unreacted fatty acid by simple precipitation. The solubility of these monoesters in *n*-heptane is likely associated with the lower melting points (especially *cis* uFAs) and unsaturation resulting a kink within the fatty acid chain, which reduces intermolecular packing compared to the saturated analogues which are solids.

Although the EtOAc : H_2O workup efficiently removed the unreacted carbohydrate (**1a**/**1b**) yielding a crude mixture of monoester product and unreacted fatty acid, preparative TLC was required to purify these liquid monoesters (**3e**, **3g**, **3h**, **3i**, **4e**, **4g**, **4h** and **4i**) or viscous solid monoesters (**3d** and **4d**) with 100% EtOAc as eluent. The use of preparative TLC generates additional silica and solvent waste and therefore represents a limitation of the present methodology from a green chemistry perspective. Hence, for large scale production and purification to avoid column chromatography, further development of efficient liquid–liquid extraction strategies is required.

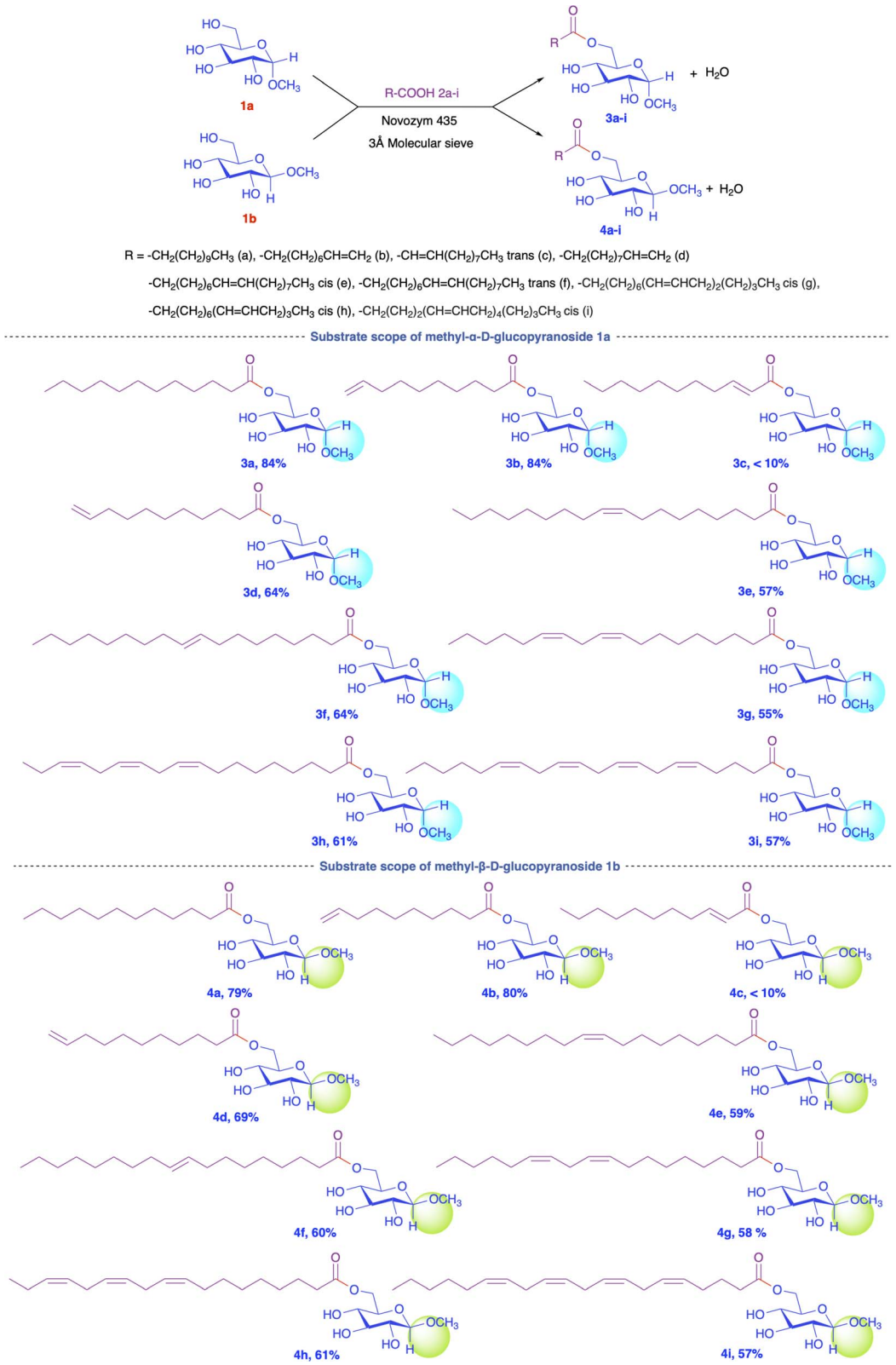

Scheme 3 Substrate scope of methyl α/β-D-glucopyranoside (**1a** and **1b**) applying the optimized reaction conditions of 1 : 3 equiv. **1a**/**1b** (85.83 mM, 0.26 mmol): fatty acids (**2a–i**), MeCN, Novozym 435 and 3 Å MS – 50 and 80 wt% of **1a**/**1b**, respectively, at 60 °C, 100 rpm for 4h.

Antimicrobial assay. The antibacterial activity of 16 tested CFAE was evaluated against a clinical isolated Gram-positive bacterium *Staphylococcus aureus* (ATCC 25923), with contrasting results observed based on fatty acid length, degree of unsaturation, geometrical isomers, and carbohydrate configuration. The minimum inhibitory concentration (MIC)

Table 5 MIC, MBC, and % inhibition values of methyl α/β-D-glucopyranoside saturated and unsaturated fatty acid esters and free fatty acids against *Staphylococcus aureus*[a]

	S. aureus (ATCC 25923)		
Compound name and label	% Inhibition[b]	MIC (mM)	MBC (mM)
Vancomycin hydrochloride	—	0.0078	0.0078
Lauric acid (**2a**)	—	0.2500	0.2500
Oleic acid (**2e**)	—	0.5000	0.5000
Methyl 6-*O*-dodecanoyl-α-D-glucopyranoside (**3a**)	—	0.0625	0.1250
Methyl 6-*O*-dodecanoyl-β-D-glucopyranoside (**4a**)	—	0.0312	0.0312
Methyl 6-*O*-9-decenoyl-α-D-glucopyranoside (**3b**)	5.28 ± 4.38 (at 0.5000 mM)	NA[c]	NA
Methyl 6-*O*-9-decenoyl-β-D-glucopyranoside (**4b**)	2.29 ± 0.03 (at 0.5000 mM)	NA	NA
Methyl 6-*O*-10-undecenoyl-α-D-glucopyranoside (**3d**)	10.25 ± 0.49 (at 0.5000 mM)	NA	NA
Methyl 6-*O*-10-undecenoyl-β-D-glucopyranoside (**4d**)	31.91 ± 5.56 (at 0.5000 mM)	NA	NA
Methyl 6-*O*-(9Z)-octadecenoyl-α-D-glucopyranoside (**3e**)	44.38 ± 11.30 (at 0.5000 mM)	NA	NA
Methyl 6-*O*-(9Z)-octadecenoyl-β-D-glucopyranoside (**4e**)	—	0.0156	0.0156
Methyl 6-*O*-(9E)-octadecenoyl-α-D-glucopyranoside (**3f**)	20.94 ± 2.96 (at 0.5000 mM)	NA	NA
Methyl 6-*O*-(9E)-octadecenoyl-β-D-glucopyranoside (**4f**)	7.20 ± 1.39 (at 0.5000 mM)	NA	NA
Methyl 6-*O*-(9Z,12Z)-octadecadienoyl-α-D-glucopyranoside (**3g**)	45.59 ± 10.85 (at 0.5000 mM)	NA	NA
Methyl 6-*O*-(9Z,12Z)-octadecadienoyl-β-D-glucopyranoside (**4g**)	—	0.5000	0.6250
Methyl 6-*O*-(9Z,12Z,15Z)-octadecatrienoyl-α-D-glucopyranoside (**3h**)	25.68 ± 4.36 (at 0.5000 mM)	NA	NA
Methyl 6-*O*-(9Z,12Z,15Z)-octadecatrienoyl-β-D-glucopyranoside (**4h**)	94.84 ± 7.61 (at 0.1250 mM)	0.2500	0.5000
Methyl 6-*O*-(5Z,8Z,11Z,14Z)-eicosatetraenoyl-α-D-glucopyranoside (**3i**)	—	0.5000	2.5000
Methyl 6-*O*-(5Z,8Z,11Z,14Z)-eicosatetraenoyl-β-D-glucopyranoside (**4i**)	62.70 ± 2.21 (at 0.2500 mM)	0.5000	0.6250

[a] Broth microdilution method was used to determine MIC & MBC values and vancomycin as positive control. MIC and MBC values are reported to four decimal places to reflect the concentration resolution used in the microdilution assay. [b] % Inhibition $= \frac{\text{Control value} - \text{Sample value}}{\text{Control value}} \times 100$, where control and sample values are bacterial growth in the absence and presence of the compounds, respectively. All % inhibition values are reported as mean ± standard deviation from triplicate measurements ($n = 3$). [c] NA = Not active, compounds with % inhibition <50% at the tested concentration of 0.5000 mM, where corresponding MIC and MBC values are considered as not active and only % inhibition values are given.

and minimum bactericidal concentration (MBC) are presented in Table 5. In the literature, the reported mode of action of CFAE involves increased permeability of the bacterial cell envelope, leading to leakage of intracellular contents and subsequent bacterial death, including *S. aureus*.[116–118] The saturated lauric acid ($C_{12:0}$) based monoesters **3a** and **4a** have previously shown significant activity against *S. aureus*.[6] In comparison with the parent fatty acid, lauric acid (**2a**), which showed MIC and MBC values of 0.2500 mM, the corresponding monoesters of α- and β-anomers *i.e.*, **3a** and **4a** exhibited MIC values of 0.0625 mM and 0.0312 mM, corresponding to approximately 4-fold and 8-fold improvements in inhibitory effect, respectively. However, the synthesized $C_{10:1}$, $C_{11:1}$ based fatty acid esters for both MAG and MBG (**3b**, **4b**, **3d** and **4d**) were inactive, suggesting the ineffectiveness of medium-chain monounsaturated fatty acid esters towards the *S. aureus* strain (ATCC 25923). For monounsaturated long chain FAs ($C_{18:1}$) of oleic acid (*cis*) and elaidic acid (*trans*), elaidic acid monoesters (**3f** and **4f**) were inactive. In contrast, the oleic acid monoester of the β-anomer (**4e**) showed highest antibacterial activity with MIC and MBC values of 0.0156 mM, respectively, corresponding to a 32-fold improvement relative to the parent fatty acid *i.e.*, oleic acid (2e), which exhibited MIC and MBC values of 0.5000 mM. In contrast the synthesised monoester of the α-anomer (**3e**) was inactive. A similar trend was observed for polyunsaturated long chain FAs of linoleic acid ($C_{18:2}$) and linolenic acid ($C_{18:3}$), where only the β-anomer monoester showed moderate activity, with MIC and MBC of 0.5000 and 0.6250 mM (**4g**), and 0.2500 and 0.5000 mM (**4h**), respectively, with the linolenic acid monoester (**4h**) being more active. Interestingly, both the α- and β-anomer of arachidonic acid ($C_{20:4}$) derived monoesters (**3i** and **4i**) have comparable MIC of 0.5000 mM; however, the β-anomer demonstrated a lower MBC of 0.6250 mM (**4i**) compared to 2.5000 mM for the α-anomer (**3i**). The clear difference between α- and β-anomers suggest that the configuration of methyl glucopyranoside may influence the bactericidal activity, potentially through differences in amphiphilic balance and interaction with the bacterial membrane, hence their disruption.

Overall, these results show that among all *cis* long chain mono- and poly-unsaturated fatty acid monoesters ($C_{18:1}$, $C_{18:2}$, $C_{18:3}$, and $C_{20:4}$) tested, the MBG-derived fatty acid monoesters (**4e**, **4g**, **4h**, and **4i**) exhibited antibacterial activity against *S. aureus* (ATCC 25923). In particular, the monounsaturated fatty acid ester of β-anomer *i.e.*, MBG monooleate (**4e**) demonstrated the strongest bacterial activity compared to the polyunsaturated MBG monoesters (**4g**, **4h**, and **4i**). It was also observed that the CFAE derivatives exhibited improved solubility compared to the corresponding free fatty acids in H_2O: organic solvent system, which may contribute to enhanced bioavailability and antibacterial activity. These findings indicate *cis*-monounsaturated FAs (oleic acid) are more active than *trans*- (elaidic acid) and β-anomer glucoside monoesters hold promising structural leads for further development of carbohydrate-based antimicrobial agents.

Conclusions

This study presents process optimization of a CALB-catalyzed synthesis of methyl glucoside fatty acid esters (CFAE). The study encompassed greener solvent screening, ^{1}H qNMR guided reaction optimization, purification strategies, waste minimization through recovery of unreacted LA and recycling of Novozym 435, substrate scope with their antimicrobial evaluation, and green metrics evaluation and a screening LCA for the gram-scale synthesis of **3a**. Propylene carbonate (PC) was identified as a promising greener solvent, with 59% yield of **3a**, however, its practical application necessitates additional work-up optimization due to solvent removal challenges. MeCN remained the highest performing solvent under optimized conditions with 89% yield. Correlation of solvent's Kamlet–Taft parameters indicated that solvents with polarizability (π^*) >0.70 and basicity (β) between 0.30–0.60 generally supported monoester yields >50%. However, this correlation has limitation, as yield trend deviates by the specific solvent-substrate and substrate–enzyme interactions.

The optimized process was successfully applied at gram-scale synthesis of **3a**, affording 83.50% isolated yield within relatively less reaction time of 4 h compared to literature. Applying the optimized conditions, substrate expansion of methyl α/β-D-glucopyranoside with medium to longer chain mono- and polyunsaturated fatty acids afforded products in <10–84% isolated yield, except for the α,β-unsaturated fatty acid (**2c**) which showed low reactivity (<10%). Antimicrobial evaluation against *S. aureus* (ATCC 25923) revealed the strongest antibacterial activity of *cis* monounsaturated β-anomer (MBG monooleate, **4e**), with MIC and MBC values of 0.0156 mM, corresponding to ∼32-fold improvement in inhibitory potency compared to the parent oleic acid (**2e**, MIC/MBC = 0.5000 mM). These findings highlight the influence of fatty-acid geometry (chain length and geometrical isomers) and glucoside configuration (α- and β-anomers) on antibacterial activity.

EcoScale evaluation yielded a score of 75.75, classifying the protocol as an excellent synthetic procedure. Novozym 435 recyclability across seven 4 h reaction batches under optimized conditions revealed a total decrease in 22.69% yield by the 7th reaction. Recovery of unreacted LA (69.30% of input) in gram-scale synthesis improved the reaction mass efficiency (RME) from 39.53% to 83.19%. The total PMI was 143.73 g g^{-1}, with solvents contributing 92.83% of total PMI, identifying solvent usage as the key area for improvement. In the screening cradle-to-gate LCA for the bench gram-scale synthesis of **3a**, electricity consumption for 3 Å molecular sieve activation was identified as the dominant hotspot, while solvent use and waste treatment were secondary contributors, with a total endpoint single score impact of 65.65 mPt. The use of proxy datasets where exact inventory data were unavailable, and gram-scale experimental data for this LCA represents a limitation of the current study.

Overall, this work provides a quantitative benchmark dataset for bench-scale CFAE synthesis and identifies improvement priorities, such as improved purification strategies, less solvent use, lower auxiliary energy consumption. It supports further investigation of carbohydrate-based fatty acid esters (CFAE) as potential antimicrobial agents. As a comprehensive assessment, it shares knowledge in the applicability of comprehensive sustainability approach at bench scale.

Author contributions

A. B., C. L., J. L. D. and M. K. designed the programme of work and A. B. conducted process development and synthesis experiments along with data analysis, C. L, J. L. D and M. K acted as supervisors to the programme. The antibacterial assessment work was conducted by L. C and S. W. A. B. wrote the original draft. C. L., J. L. D., M. K., L. C. and S. J. reviewed, edited the draft. All authors have given approval to the final version of the manuscript.

Conflicts of interest

The authors declare no conflicts of interest.

Data availability

Data supporting this article has been included in the supplementary information (SI). Supplementary information: experimental data, reaction optimization data, substrate scope, product characterization data, antimicrobial evaluation data, green metrics/LCA inventory details, and the accompanying CHEM21 First-Pass Toolkit analysis spreadsheet. See DOI: https://doi.org/10.1039/d6su00302h.

Acknowledgements

The authors are grateful for the PhD scholarship funded by the South East Technological University PhD Scholarship Programme (WD_2020_60_WSCH). The authors wish to thank senior technical officer Aidan Sinnott for support within the laboratory.

References

1 S.-H. Pyo, J. Chen, R. Ye and D. G. Hayes, in *Biobased Surfactants*, ed. D. G. Hayes, D. K. Y. Solaiman and R. D. Ashby, AOCS Press, 2nd edn, 2019, pp. 325–363, DOI: 10.1016/B978-0-12-812705-6.00010-1.
2 B. Pérez, S. Anankanbil and Z. Guo, in *Fatty Acids*, ed. M. U. Ahmad, AOCS Press, 2017, pp. 329–354, DOI: 10.1016/B978-0-12-809521-8.00010-6.
3 E. Zago, N. Joly, L. Chaveriat, V. Lequart and P. Martin, *Biotechnol. Rep.*, 2021, **30**, e00631.
4 A. Spalletta, N. Joly and P. Martin, *Int. J. Mol. Sci.*, 2024, **25**, 3727.
5 M. N. AlFindee, Q. Zhang, Y. P. Subedi, J. P. Shrestha, Y. Kawasaki, M. Grilley, J. Y. Takemoto and C.-W. T. Chang, *Bioorg. Med. Chem.*, 2018, **26**, 765–774.
6 A. Smith, P. Nobmann, G. Henehan, P. Bourke and J. Dunne, *Carbohydr. Res.*, 2008, **343**, 2557–2566.

7 A. Perona, P. Hoyos, L. A. Ticona, C. García-Oliva, A. Merchán and M. J. Hernáiz, *Catal. Today*, 2024, **433**, 114623.
8 H. A. El-Baz, A. M. Elazzazy, T. S. Saleh, M. Dourou, J. A. Mahyoub, M. N. Baeshen, H. R. Madian and G. Aggelis, *Appl. Sci.*, 2021, **11**, 2700.
9 V. Giorgi, E. Botto, C. Fontana, L. Della Mea, S. Vaz Jr, P. Menéndez and P. Rodríguez, *Catalysts*, 2022, **12**, 610.
10 R. Hollenbach, A. Delavault, L. Gebhardt, H. Soergel, C. Muhle-Goll, K. Ochsenreither and C. Syldatk, *ACS Sustain. Chem. Eng.*, 2022, **10**, 10192–10202.
11 K. Ren, G. Chen, Z. Zhang, Z. Long, B. Zhou, W. Han and Q. Lin, *Food Chem.*, 2025, **27**, 102383.
12 S. J. Marathe, N. Dedhia and R. S. Singhal, *Curr. Opin. Food Sci.*, 2022, **43**, 163–173.
13 P. T. Anastas and J. C. Warner, *Green Chemistry: Theory and Practice*, Oxford University Press, 2000.
14 R. J. Giraud, P. A. Williams, A. Sehgal, E. Ponnusamy, A. K. Phillips and J. B. Manley, *ACS Sustain. Chem. Eng.*, 2014, **2**, 2237–2242.
15 A. Spalletta, N. Joly and P. Martin, *Chemistry*, 2023, **5**, 1855–1869.
16 P. Hoyos, V. Cabanas, C. Garcia-Oliva, J. Pena and M. J. Hernaiz, *ACS Sustain. Chem. Eng.*, 2024, **12**, 12421–12429.
17 R. Semproli, S. N. Chanquia, J. P. Bittner, S. Müller, P. Domínguez de María, S. Kara and D. Ubiali, *ACS Sustain. Chem. Eng.*, 2023, **11**, 5926–5936.
18 W. Gładkowski, A. Chojnacka, A. Włoch, H. Pruchnik, A. Grudniewska, A. Dunal, A. Dudek, G. Maciejewska and M. Rudzińska, *ChemPlusChem*, 2023, **88**, e202300161.
19 G. R. List and J. W. King, *Hydrogenation of Fats and Oils: Theory and Practice*, Elsevier, 2015.
20 S. T. Akula, A. Nagaraja, M. Ravikanth, N. G. R. Kumar, Y. Kalyan and D. Divya, *Biomed. Biotechnol. Res. J.*, 2021, **5**, 229–234.
21 D. Arcens, E. Grau, S. Grelier, H. Cramail and F. Peruch, *Mol. Catal.*, 2018, **460**, 63–68.
22 C. Jia, J. Zhao, B. Feng, X. Zhang and W. Xia, *J. Mol. Catal. B: Enzym.*, 2010, **62**, 265–269.
23 F. Fischer, M. Happe, J. Emery, A. Fornage and R. Schütz, *J. Mol. Catal. B: Enzym.*, 2013, **90**, 98–106.
24 W. Zhang, Y. Wang, K. Hayat, X. Zhang, A. Shabbar, B. Feng and C. Jia, *Biotechnol. Lett.*, 2009, **31**, 423–428.
25 V. M. Pappalardo, C. G. Boeriu, F. Zaccheria and N. Ravasio, *Mol. Catal.*, 2017, **433**, 383–390.
26 M. Ferrer, G. Perez, F. J. Plou, J. V. Castell and A. Ballesteros, *Biotechnol. Appl. Biochem.*, 2005, **42**, 35–39.
27 E. Abdulmalek, N. F. Hamidon and M. B. Abdul Rahman, *J. Mol. Catal. B: Enzym.*, 2016, **132**, 1–4.
28 D. An, X. Zhang, F. Liang, M. Xian, D. Feng and Z. Ye, *Colloids Surf. A Physicochem. Eng. Asp.*, 2019, **577**, 257–264.
29 A. M. Gumel, M. S. M. Annuar, T. Heidelberg and Y. Chisti, *Process Biochem.*, 2011, **46**, 2079–2090.
30 E. Abdulmalek, H. S. Mohd Saupi, B. A. Tejo, M. Basri, A. B. Salleh, R. N. Z. Raja Abd Rahman and M. B. Abdul Rahman, *J. Mol. Catal. B: Enzym.*, 2012, **76**, 37–43.
31 A. Favrelle, C. Boyère, P. Laurent, G. Broze, C. Blecker, M. Paquot, C. Jérôme and A. Debuigne, *Carbohydr. Res.*, 2011, **346**, 1161–1164.
32 Y. Gu and F. Jérôme, *Chem. Soc. Rev.*, 2013, **42**, 9550–9570.
33 I. T. Horváth and P. T. Anastas, *Chem. Rev.*, 2007, **107**, 2169–2173.
34 S. Kar, H. Sanderson, K. Roy, E. Benfenati and J. Leszczynski, *Chem. Rev.*, 2021, **122**, 3637–3710.
35 M. C. Bryan, P. J. Dunn, D. Entwistle, F. Gallou, S. G. Koenig, J. D. Hayler, M. R. Hickey, S. Hughes, M. E. Kopach, G. Moine, P. Richardson, F. Roschangar, A. Steven and F. J. Weiberth, *Green Chem.*, 2018, **20**, 5082–5103.
36 A. Jordan, C. G. J. Hall, L. R. Thorp and H. F. Sneddon, *Chem. Rev.*, 2022, **122**, 6749–6794.
37 R. J. Kelly, *Chem. Health Saf.*, 1996, **3**, 28–36.
38 G. Trapasso and F. Aricò, *Green Chem.*, 2025, **27**, 6925–6966.
39 K. Watanabe, N. Yamagiwa and Y. Torisawa, *Org. Process Res. Dev.*, 2007, **11**, 251–258.
40 V. Pace, P. Hoyos, L. Castoldi, P. Domínguez de María and A. R. Alcántara, *ChemSusChem*, 2012, **5**, 1369–1379.
41 Y. Simeó, J. V. Sinisterra and A. R. Alcántara, *Green Chem.*, 2009, **11**, 855–862.
42 A. Yamaguchi, O. Sato, N. Mimura and M. Shirai, *Catal. Commun.*, 2015, **67**, 59–63.
43 I. T. Horváth, H. Mehdi, V. Fábos, L. Boda and L. T. Mika, *Green Chem.*, 2008, **10**, 238–242.
44 N. A. Stini, P. L. Gkizis and C. G. Kokotos, *Green Chem.*, 2022, **24**, 6435–6449.
45 N. Guajardo and P. Domínguez de María, *Mol. Catal.*, 2020, **485**, 110813.
46 S. Chemat, V. Tomao and F. Chemat, in *Green Solvents I: Properties and Applications in Chemistry*, ed. A. Mohammad, Springer Netherlands, Dordrecht, 2012, pp. 175–186, DOI: 10.1007/978-94-007-1712-1_5.
47 Y.-Z. Qin, M.-H. Zong, W.-Y. Lou and N. Li, *ACS Sustain. Chem. Eng.*, 2016, **4**, 4050–4054.
48 H. Cumming and S. N. Marshall, *J. Biotechnol.*, 2021, **325**, 217–225.
49 K. H. Zhao, Y. Z. Cai, X. S. Lin, J. Xiong, P. J. Halling and Z. Yang, *Molecules*, 2016, 21.
50 P. Degn and W. Zimmermann, *Biotechnol. Bioeng.*, 2001, **74**, 483–491.
51 M. F. K. Ariffin, M. S. M. Annuar and T. Heidelberg, *J. Surfactants Deterg.*, 2014, **17**, 683–692.
52 J. Mutschler, T. Rausis, J.-M. Bourgeois, C. Bastian, D. Zufferey, I. V. Mohrenz and F. Fischer, *Green Chem.*, 2009, **11**, 1793–1800.
53 A. Nayak, J. Dunne, M. Kinsella and C. M. Lennon, *Carbohydr. Res.*, 2024, **540**, 109143.
54 S. K. Bharti and R. Roy, *Trac. Trends Anal. Chem.*, 2012, **35**, 5–26.
55 G. F. Pauli, S.-N. Chen, C. Simmler, D. C. Lankin, T. Gödecke, B. U. Jaki, J. B. Friesen, J. B. McAlpine and J. G. Napolitano, *J. Med. Chem.*, 2014, **57**, 9220–9231.

56 CHEM21, Chemical Manufacturing Methods for the 21st Century Pharmaceutical Industries, https://www.chem21.eu/, October 2024.
57 K. Van Aken, L. Strekowski and L. Patiny, *Beilstein J. Org. Chem.*, 2006, **2**, 3.
58 M. L. Parisi, A. Dessì, L. Zani, S. Maranghi, S. Mohammadpourasl, M. Calamante, A. Mordini, R. Basosi, G. Reginato and A. Sinicropi, *Front. Chem.*, 2020, 8–2020.
59 R. Mathew, S. Chen, A. Brandt-Talbot, J. S. Edge and T. Welton, *Green Chem.*, 2026, **28**, 6404–6422.
60 F. Björkling, S. E. Godtfredsen and O. Kirk, *J. Chem. Soc. Chem. Commun.*, 1989, 934–935, DOI: 10.1039/C39890000934.
61 M. P. de Nijs, L. Maat and A. P. G. Kieboom, *Recl. Trav. Chim. Pays-Bas*, 1990, **109**, 429–433.
62 K. Adelhorst, F. Björkling, S. E. Godtfredsen and O. Kirk, *Synthesis*, 1990, 112–115.
63 O. Kirk, F. Björkling, S. E. Godtfredsen and T. O. Larsen, *Biocatalysis*, 1992, **6**, 127–134.
64 M. Gelo-Pujic, E. Guibé-Jampel, A. Loupy, S. A. Galema and D. Mathé, *J. Chem. Soc. Perkin Trans.*, 1996, **1**, 2777–2780, DOI: 10.1039/P19960002777.
65 M.-P. Bousquet, R.-M. Willemot, P. Monsan and E. Boures, *Biotechnol. Bioeng.*, 1999, **63**, 730–736.
66 S. Westwood, T. Yamazaki, T. Huang, B. Garrido, I. Ün, W. Zhang, G. Martos, N. Stoppacher, T. Saito and R. Wielgosz, *Metrologia*, 2019, **56**, 064001.
67 L. M. i. Canals, A. Azapagic, G. Doka, D. Jefferies, H. King, C. Mutel, T. Nemecek, A. Roches, S. Sim and H. Stichnothe, *J. Ind. Ecol.*, 2011, **15**, 707–725.
68 V. Subramanian and J. S. Golden, *J. Clean. Prod.*, 2016, **115**, 354–361.
69 S. Jaiswal, B. Duffy, A. K. Jaiswal, N. Stobie and P. McHale, *Int. J. Antimicrob. Agents*, 2010, **36**, 280–283.
70 S. Jaiswal, P. McHale and B. Duffy, *Colloids Surf. B Biointerfaces*, 2012, **94**, 170–176.
71 D. Prat, A. Wells, J. Hayler, H. Sneddon, C. R. McElroy, S. Abou-Shehada and P. J. Dunn, *Green Chem.*, 2016, **18**, 288–296.
72 C. M. Alder, J. D. Hayler, R. K. Henderson, A. M. Redman, L. Shukla, L. E. Shuster and H. F. Sneddon, *Green Chem.*, 2016, **18**, 3879–3890.
73 A. R. Go, Y. Lee, Y. H. Kim, S. Park, J. Choi, J. Lee, S. O. Han, S. W. Kim and C. Park, *Enzyme Microb. Technol.*, 2013, **53**, 154–158.
74 M. Selva, A. Perosa, D. Rodríguez-Padrón and R. Luque, *ACS Sustain. Chem. Eng.*, 2019, **7**, 6471–6479.
75 X.-M. Wu, W. Sun, J.-Y. Xin and C.-G. Xia, *World J. Microbiol. Biotechnol.*, 2008, **24**, 2421–2424.
76 J. S Bello Forero, J. A Hernández Muñoz, J. Jones Junior and F. M da Silva, *Curr. Org. Synth.*, 2016, **13**, 834–846.
77 P. G. Jessop, D. A. Jessop, D. Fu and L. Phan, *Green Chem.*, 2012, **14**, 1245–1259.
78 M. Wu, F. Wu, H. L. Luan and R. J. Chen, *Clin. Chim. Acta*, 2005, **63**, 787–790.
79 ChemSpider, https://www.chemspider.com/, accessed April 2026.
80 J. Sherwood, M. De bruyn, A. Constantinou, L. Moity, C. R. McElroy, T. J. Farmer, T. Duncan, W. Raverty, A. J. Hunt and J. H. Clark, *Chem. Commun.*, 2014, **50**, 9650–9652.
81 A. Damjanoska, K. Mitreska, M. Petrova, J. Acevska, K. Brezovska and N. Nakov, *Molecules*, 2025, **30**, 2713.
82 C. Reichardt, *Chem. Rev.*, 1994, **94**, 2319–2358.
83 C. Laane, S. Boeren, K. Vos and C. Veeger, *Biotechnol. Bioeng.*, 1987, **30**, 81–87.
84 J. Sherwood, H. L. Parker, K. Moonen, T. J. Farmer and A. J. Hunt, *Green Chem.*, 2016, **18**, 3990–3996.
85 W. M. Haynes, *CRC Handbook of Chemistry and Physics*, CRC press, 2016.
86 A. K. El-Deen and K. Shimizu, *Anal. Sci.*, 2019, **35**, 1385–1391.
87 L. Cao, U. T. Bornscheuer and R. D. Schmid, *J. Mol. Catal. B: Enzym.*, 1999, **6**, 279–285.
88 M. J. Kamlet, J. L. M. Abboud, M. H. Abraham and R. W. Taft, *J. Org. Chem.*, 1983, **48**, 2877–2887.
89 H. P. Tai and G. Brunner, *J. Supercrit. Fluids*, 2009, **48**, 36–40.
90 Y. Watanabe, Y. Miyawaki, S. Adachi, K. Nakanishi and R. Matsuno, *Enzyme Microb. Technol.*, 2001, **29**, 494–498.
91 J. A. Arcos, C. G. Hill Jr and C. Otero, *Biotechnol. Bioeng.*, 2001, **73**, 104–110.
92 L. Cao, U. T. Bornscheuer and R. D. Schmid, *Fett/Lipid*, 1996, **98**, 332–335.
93 S. C. Kim, Y. H. Kim, H. Lee, D. Y. Yoon and B. K. Song, *J. Mol. Catal. B: Enzym.*, 2007, **49**, 75–78.
94 G. V. Waghmare, M. D. Vetal and V. K. Rathod, *Ultrason. Sonochem.*, 2015, **22**, 311–316.
95 Y. Zhang, Z. Yuan, B. Hu, J. Deng, Q. Yao, X. Zhang, X. Liu, Y. Fu and Q. Lu, *Green Chem.*, 2019, **21**, 812–820.
96 E. C. Corker, U. V. Mentzel, J. Mielby, A. Riisager and R. Fehrmann, *Green Chem.*, 2013, **15**, 928–933.
97 A. B. Lutjen, M. A. Quirk and E. M. Kolonko, *J. Vis. Exp.*, 2018, e58803.
98 F. Cauglia and P. Canepa, *Bioresour. Technol.*, 2008, **99**, 4065–4072.
99 C. C. Akoh and L. N. Mutua, *Enzyme Microb. Technol.*, 1994, **16**, 115–119.
100 C. Ortiz, M. L. Ferreira, O. Barbosa, J. C. S. dos Santos, R. C. Rodrigues, Á. Berenguer-Murcia, L. E. Briand and R. Fernandez-Lafuente, *Catal. Sci. Technol.*, 2019, **9**, 2380–2420.
101 R. M. Daniel, J. L. Finney, M. Stoneham and P. J. Halling, *Phil. Trans. Roy. Soc. Lond. B Biol. Sci.*, 2004, **359**, 1287–1297.
102 Brasil, RDC no 166 de 24 de julho de 2017, Agência Nacional de Vigilância Sanitária, Brasília, 2017, https://antigo.anvisa.gov.br/documents/10181/2721567/RDC_166_2017_COMP.pdf/d5fb92b3-6c6b-4130-8670-4e3263763401.
103 K. Rai, P. Potphode, C. Gupta and N. Rao, *Int. J. Res. Pharm. Chem.*, 2020, **10**, 173–190.

104 V. Vescovi, W. Kopp, J. M. Guisán, R. L. Giordano, A. A. Mendes and P. W. Tardioli, *Process Biochem.*, 2016, **51**, 2055–2066.
105 C. Garcia-Galan, Á. Berenguer-Murcia, R. Fernandez-Lafuente and R. C. Rodrigues, *Adv. Synth. Catal.*, 2011, **353**, 2885–2904.
106 J. C. S. d. Santos, O. Barbosa, C. Ortiz, A. Berenguer-Murcia, R. C. Rodrigues and R. Fernandez-Lafuente, *ChemCatChem*, 2015, **7**, 2413–2432.
107 J. J. Virgen-Ortíz, V. G. Tacias-Pascacio, D. B. Hirata, B. Torrestiana-Sanchez, A. Rosales-Quintero and R. Fernandez-Lafuente, *Enzyme Microb. Technol.*, 2017, **96**, 30–35.
108 C. R. McElroy, A. Constantinou, L. C. Jones, L. Summerton and J. H. Clark, *Green Chem.*, 2015, **17**, 3111–3121.
109 R. Villa, F. J. Ruiz, F. Velasco, S. Nieto, R. Porcar, E. Garcia-Verdugo and P. Lozano, *ACS Sustain. Chem. Eng.*, 2024, **12**, 15033–15043.
110 S. Nieto, J. M. Bernal, R. Villa, E. Garcia-Verdugo, A. Donaire and P. Lozano, *ACS Sustain. Chem. Eng.*, 2023, **11**, 5737–5747.
111 E. R. Monteith, P. Mampuys, L. Summerton, J. H. Clark, B. U. W. Maes and C. R. McElroy, *Green Chem.*, 2020, **22**, 123–135.
112 H. H. Khoo, V. Isoni and P. N. Sharratt, *Sustain. Prod. Consum.*, 2018, **16**, 68–87.
113 F. Piccinno, R. Hischier, S. Seeger and C. Som, *J. Clean. Prod.*, 2016, **135**, 1085–1097.
114 T. Kobayashi, S. Adachi and R. Matsuno, *Biotechnol. Lett.*, 2003, **25**, 3–7.
115 T. Kobayashi, *Biotechnol. Lett.*, 2011, **33**, 1911–1919.
116 P. Nobmann, P. Bourke, J. Dunne and G. Henehan, *J. Appl. Microbiol.*, 2010, **108**, 2152–2161.
117 L. Zhao, H. Zhang, T. Hao and S. Li, *Food Chem.*, 2015, **187**, 370–377.
118 M. Ferrer, J. Soliveri, F. J. Plou, N. López-Cortés, D. Reyes-Duarte, M. Christensen, J. L. Copa-Patiño and A. Ballesteros, *Enzyme Microb. Technol.*, 2005, **36**, 391–398.